European Journal of Medicinal Chemistry 68 (2013) 270–283

Contents lists available at SciVerse ScienceDirect

European Journal of Medicinal Chemistry

journal homepage: http://www.elsevier.com/locate/ejmech

Original article

Discovery of pyrazole as C-terminus of selective BACE1 inhibitors

Yiquan Zou [a,1], Lei Xu [b,1], Wuyan Chen [a], Yiping Zhu [a], Tiantian Chen [a], Yan Fu [a], Li Li [a], Lanping Ma [a], Bing Xiong [a], Xin Wang [a], Jian Li [c], Jianhua He [c], Haiyan Zhang [a,*], Yechun Xu [a,*], Jia Li [b,*], Jingkang Shen [a,*]

[a] State Key Laboratory of Drug Research, Shanghai Institute of Materia Medica, Chinese Academy of Sciences, 555 Zuchongzhi Road, Shanghai 201203, PR China
[b] The National Center for Drug Screening, 189 Guoshoujing Road, Shanghai 201203, PR China
[c] Shanghai Institute of Applied Physics, Chinese Academy of Sciences, 239 Zhang Heng Road, Pudong New District, Shanghai 201203, PR China

ARTICLE INFO

Article history:
Received 7 November 2012
Received in revised form
26 April 2013
Accepted 6 June 2013
Available online 21 June 2013

Keywords:
Alzheimer's disease
BACE1
C-terminus
Click chemistry
In situ screening assay
Pyrazole

ABSTRACT

We recently discovered and reported dual inhibitor **5** of AChE and BACE1 with *N*-benzylpiperidine ethyl as C-terminus. Compound **5** showed potent inhibitory activities for BACE1, and could reduce endogenous $A\beta_{1-40}$ production in APP transgenic mice. In present work, we rapidly identified substituted triazole as the C-terminus of compound **5** by replacing the benzylpiperidine ethyl group with click chemistry and tested these synthesized compounds by *in situ* screening assay. As revealed by the crystal structures of BACE1 in complex with our triazole compound **12**, we found that Pro70 and Thr72 located in the flap region were the critical components for binding with these inhibitors. With the aid of the crystal structure, a new series of five-membered heterocyclic compounds was prepared in order to explore the structure–activity relationship (SAR) of this class of molecules. From these efforts, pyrazole was discovered as a novel C-terminus of BACE1 inhibitors. After further modification of pyrazole with variable substituents, compound **37** exhibited good potency in enzyme inhibition assay (IC_{50} = 0.025 μM) and compound **33** showed moderate inhibition effects on Aβ production of APP transfected HEK293 cells. Moreover, these pyrazole derivatives demonstrated good selectivity versus cathepsin D. Our results indicated that the vicinity of Pro70 and Thr72 might be utilized as a subsite, and the discovered pyrazole derivatives might provide useful hints for developing novel BACE1 inhibitors as anti-AD drugs.

1. Introduction

Alzheimer's disease (AD), a form of senile dementia, is characterized by a progressive loss of memory and cognitive ability, now affecting more than 35 million elderly people worldwide with skyrocketing healthcare costs far exceeding $100 billion annually [1]. The pathology of this neurodegenerative disorder usually manifests itself with the presence of extraneuronal aggregation of plaques composed of β-amyloid peptides (Aβ) [2]. Aβ is derived from sequentially proteolytic cleavage of the β-amyloid precursor protein (β-APP) by two aspartic acid proteases, referred as β- and γ-secretase, respectively [3]. Since γ-secretase also cleaves other transmembrane proteins, such as Notch, which is involved in cell differentiation [4] thus chronic high doses of γ-secretase inhibitors may disrupt Notch-mediated processes in the gastrointestinal tract, spleen, and thymus, leading to potential mechanism-based toxicity. In contrast, Notch inhibition is not expected for β-secretase (β-site amyloid precursor protein cleaving enzyme 1; BACE1) inhibitors. Moreover, BACE1 has been identified as the rate-limiting enzyme for Aβ production [3] and BACE1 knockout homozygote mice show complete absence of Aβ production and have no reported side effects [5–7]. Therefore, BACE1 is considered as a promising target for developing drugs to treat and/or prevent AD [8].

However, development of agents capable of inhibiting the BACE1 activity has been proved to be difficult due to the large binding groove of the enzyme. According to the geometry of the long binding groove of BACE1 and the original peptide inhibitors which mimic the sequence pattern of substrate APP [9], BACE1 inhibitors were in general subdivided into three regions: an N-terminal portion, a central core and a C-terminus. In the last decade, these sections were individually subjected to modification

Abbreviations: EDCl, *N*-(3-dimethylaminopropyl)-*N*′-ethylcarbodiimide hydrochloride; HOBt, *N*-hydroxybenzotriazole; DIPEA, *N*,*N*-diisopropylethylamine; DMF, *N*,*N*-dimethylformamide; EtOAc, ethyl acetate; DCM, dichloromethane; THF, tetrahydrofuran.

* Corresponding authors. Tel.: +86 21 50806600x5407; fax: +86 21 50807088.
E-mail addresses: hzhang@mail.shcnc.ac.cn (H. Zhang), ycxu@mail.shcnc.ac.cn (Y. Xu), jli@mail.shcnc.ac.cn (J. Li), jkshen@mail.shcnc.ac.cn (J. Shen).

[1] These two authors contributed equally to this work.

0223-5234/$ – see front matter © 2013 Elsevier Masson SAS. All rights reserved.
http://dx.doi.org/10.1016/j.ejmech.2013.06.027

for reducing the peptidic characters. Many efforts have devoted to find better inhibitors [10], such as via high throughput screening, fragment-based drug discovery and virtual screening. Among them, the peptide mimic inhibitors were extensively studies. Although the N-terminus and central core parts which bound to the hydrophobic S1, S3 and polar S2, S4 subpockets had been optimized extensively (Fig. 1) [11–15], the C-terminus, occupied polar S1′, S2′, S3′, S4′ subpocket, which could hold various sizes and where different polar groups were rarely explored.

Recently, we have developed a novel series of dual inhibitors of AChE and BACE1 through introducing *N*-benzylpiperidine moiety of donepezil at C-terminus. These inhibitors exhibited good BACE1 inhibitory potency in enzymatic assay, and also showed good inhibitory effects on Aβ production of APP transfected HEK293 cells and mild protective effect against hydrogen peroxide (H_2O_2)-induced PC12 cell injury [15]. This previous study demonstrated that the C-terminus was also a critical component in BACE1 inhibitors and spurred us to explore more novel functional groups acting as C-terminus of BACE1 inhibitor. To easily track the improvement from C-terminus of inhibitors, we kept the N-terminus of compound **5** and a facile central core (Fig. 2). By utilizing click reaction and *in situ* screening assay, we could quickly assemble the effective fragments and screen the combined compounds (**10**–**17**) efficiently. Through this technology, we obtained the novel 1,2,3-triazole inhibitors which displayed potent inhibitory effects toward BACE1 and good selectivity over cathepsin D (Table 1). As revealed by the crystal structures of BACE1 in complex with compound **12**, Pro70 and Thr72 in the flap region were important for the binding interactions of these inhibitors. To elaborate the

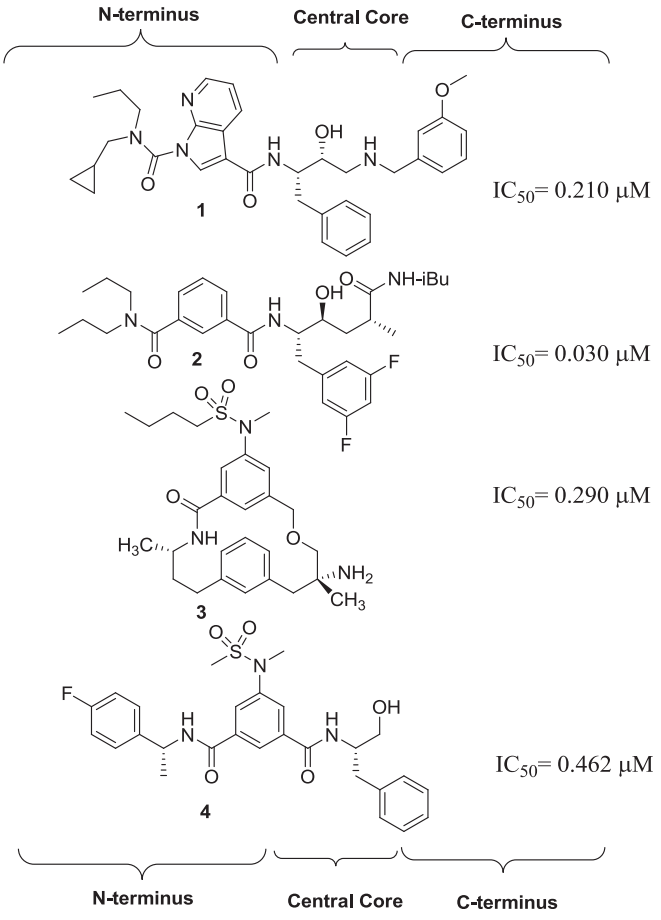

Fig. 1. Representative optimized N-terminus of BACE1 inhibitors (**1**–**4**).

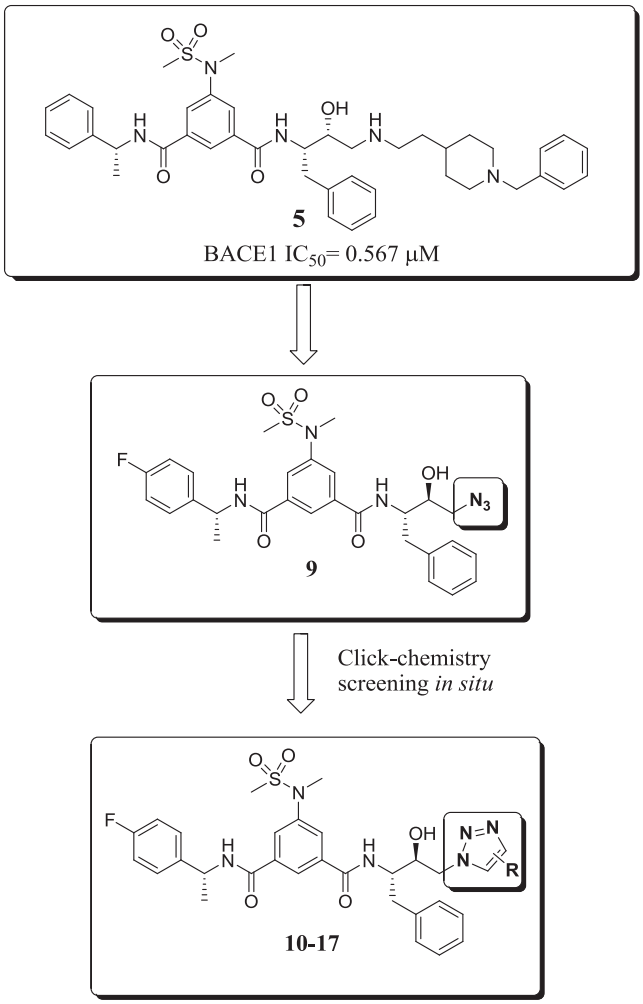

Fig. 2. Click chemistry combined with *in situ* screening approach for discovering β-secretase inhibitors.

structure–activity relationship (SAR) of C-terminus and improve the cellular activity, we replaced triazole with other five-membered heterocycles (compound **20**–**24**). Verified by the crystal structure of BACE1 in complex with compound **20** and **28** and SAR, we found pyrazole derivatives showed potent activities in BACE1 enzymatic assay, good inhibitory effects on Aβ production of APP transfected HEK293 cells and good selectivity over cathepsin D. Herein, we displayed the discovery of pyrazole as novel C-terminus of BACE1 inhibitors which might be beneficial for developing novel selective BACE1 inhibitors as anti-AD drugs.

2. Results and discussion

2.1. Chemistry

The initial compounds (**10**–**17**) were synthesized by click reaction [16]. The Huisgen Cu(I)-catalyzed alkyne-azide cycloaddition (CuAAC, a paradigm of click chemistry) had become a widely used strategy for chemical space exploration in drug design [17]. The synthetic appeal of click reaction relied upon their high yields, simple reaction conditions, tolerance of oxygen and water, and simple product isolation [18]. The Cu(I)-catalyzed 1,3-dipolar cycloaddition reaction between an organic azide and a terminal alkyne would create 1,2,3-triazole derivatives. The synthesis of intermediate azide compound **9** was shown in Scheme 1, and the

Table 1
BACE1, cathepsin D enzyme data and HEK239 cellular-inhibitory activities of compounds **10**–**17**.

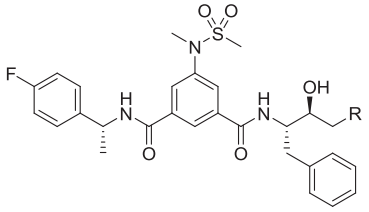

Comp.	R	BACE1 *in situ*-inhibition (%) at 1 μM[a]	BACE1 IC_{50}[b] (μM)	CatD IC_{50}[b] (μM)	HEK239-inhibition %[c] (at 10 μM)
10		ND[d]	1.800 ± 0.105	>30	9.81
11	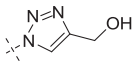	69.21	0.099 ± 0.011	>30	12.01
12	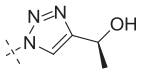	88.74	0.036 ± 0.005	>30	13.24
13	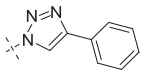	97.86	0.264 ± 0.030	10.56 ± 0.91	15.81
14	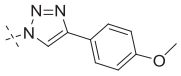	83.13	0.442 ± 0.027	13.64 ± 0.77	8.88
15	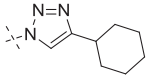	90.53	1.176 ± 0.120	12.56 ± 0.84	10.93
16	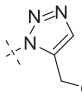	98.01	1.890 ± 0.154	>30	2.08
17	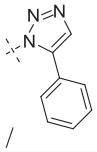	14.73	>30	>30	8.36
OM99-2	/	ND	0.071 ± 0.005	ND	ND

[a] The purity of all the *in situ* compounds were tested by HPLC and ensured the value >75%, and all inhibitory values are means of at least three separate experiments.
[b] All the IC_{50} values are tested after the compounds were purified and ensured the purity >98%, and IC_{50} values are means of at least three separate experiments.
[c] All inhibitory values are means of at least three separate experiments.
[d] 'ND' means the IC_{50} were not determined.

general synthesis of the combined molecules **10**–**17** was outlined in Scheme 2.

To prepare compounds (**10**–**17**) for *in situ* assay, 0.4 mL THF and 0.1 mL H_2O were added to each well of a 96-well plate, followed by adding the azide compound **9** (14.5 mg, 0.025 mmol) and a terminal alkyne (0.1 mmol) gradually. After shaking a few minutes, sodium ascorbate (1 mg, 0.005 mmol) and CuI (0.5 mg, 0.0025 mmol) was added into each well. Then the plate was further been shaking in shaker for 12 h at 50 °C [19]. TLC/HPLC was used to examine the accomplishment of reactions, and the identity of the resulting compounds was confirmed by LC-MS analysis of the crude reaction mixtures. After identification, the reaction solution was concentrated and the residues were used to screen straightly without further purification.

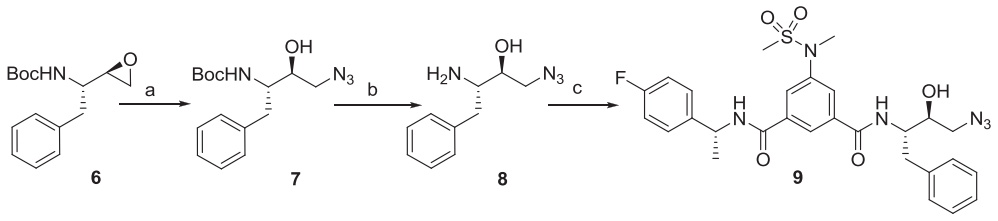

Scheme 1. Synthesis of compound **9**. Reagents and conditions: (a) NaN_3, NH_4Cl, MeOH, reflux overnight; (b) TFA/DCM = 1/4; (c) EDCI, HOBt, DIPEA, DMF, r.t. overnight.

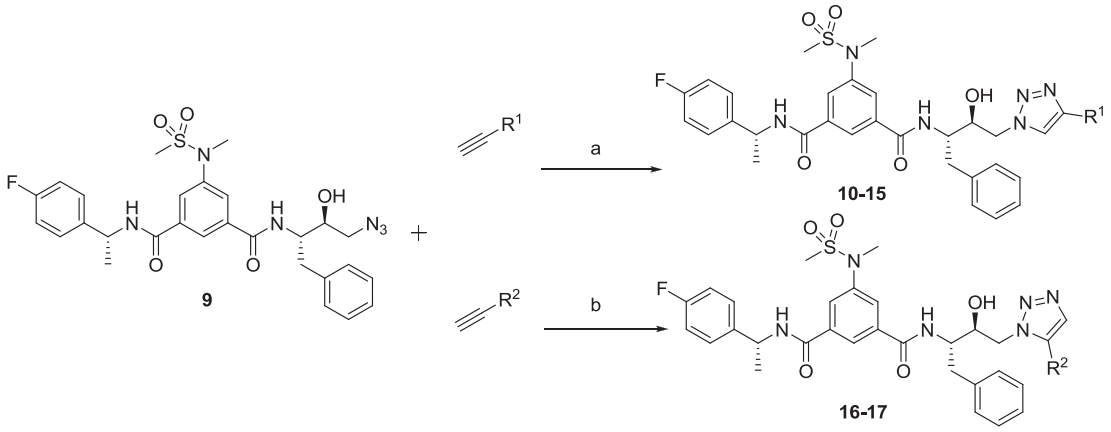

Scheme 2. Synthesis of compounds (**10**–**17**). Reagents and conditions: (a) CuI, sodium ascorbate, THF/H_2O = 4/1, 50 °C; (b) $Ru(PhP_3)_3Cl_2$, THF, 50 °C.

All bioactive compounds identified in *in situ* assay were resynthesized individually for verification with spectra characterization and further enzymatic studies. Commercially available *tert*-butyl (*S*)-1-((*R*)-oxiran-2-yl)-2-phenylethyl carbamate (compound **6**) was reacted with sodium azide in methanol to give *tert*-butyl (2*S*,3*S*)-4-azido-3-hydroxy-1-phenylbutan-2-yl carbamate (compound **7**) in good yield. Then removing the *N*-Boc group of azide compound **7** was conducted in the presence of 30% TFA in DCM, and the resulting amine (compound **8**) was subsequently reacted with 3-[(*R*)-1-(4-fluorophenyl)ethylaminocarbonyl]-5-[methyl (methylsulfonyl)amino]benzoic acid using EDCI and HOBt as the coupling agents to yield compound **9** [15]. The azide compound, a terminal alkyne, sodium ascorbate, and CuI were stirred for 12 h at 50 °C. TLC/HPLC was employed to examine the accomplishment of reactions. After examination, the reaction was concentrated *in vacuum* to afford the crude 4-substituted 1,2,3-triazole products (compounds **10**–**15**). The 5-substituted 1,2,3-triazole compounds (compounds **16**–**17**) were obtained in the presence of $Ru(PPh_3)_2Cl_2$ with moderate yields.

The general synthesis of triazole analogs **20**–**24** was outlined in Scheme 3 (the structure of compounds **20**–**24** was reported in Table 2).

Epoxide opening in sealed tube at 100 °C for 1 h afforded the Boc-protected amino alcohol, which were then deprotected under acidic conditions and underwent amide coupling to provide compounds **20**–**24** (Table 2).

Similarly, pyrazole derivatives were obtained from epoxide (compound **6**) opening in sealed tube at 100 °C for 1 h afforded the Boc-protected amino alcohol, which were then deprotected under acidic conditions and underwent amide coupling to provide compound **28**, then hydrolysis under basic conditions and underwent amide coupling provide compounds **30**–**37** (Scheme 4, Table 3).

2.2. *In situ* screening assay and SAR of triazole derivatives

The click reaction product in each well was diluted with 10% DMSO aqueous solution to 1 μM into another 96-well microtiter plate and assayed for their inhibition activity against BACE1. Compound OM99-2 (one of the earliest inhibitors discovered by Ghosh et al.) was used as the control [9]. The inhibitory activities of 1,2,3-triazoles against BACE1 were summarized in Table 1.

As shown in Table 1, all compounds showed certain BACE1 inhibitory activities. It was displayed that the triazole scaffold was suitable for the C-terminal substitution of the BACE1 inhibitor. Comparison of the active compounds indicated that, the polar S1′–S2′ pockets of BACE1 could hold various kinds of substituents, but the size and the property of substituents on the 1,2,3-triazole were crucial for the potency. Compound **10**, which has not any substituent on the 1,2,3-triazole, displayed moderate inhibitory potency (IC_{50} = 1.800 μM). Small hydrophilic groups substituted at the 4-substituted 1,2,3-triazole (**11** and **12**) led to more substantial increase in potency than those with large hydrophobic groups such as phenyl, 4-methoxy phenyl, and cyclohexyl (compounds **13**, **14**, and **15** respectively). When introduced the hydroxymethyl or phenyl group into 5-position of triazole, respectively compounds **16** and **17** displayed weak activities against BACE1. Moreover, by comparing compound **10** (IC_{50} = 1.800 μM) and compound **11** (IC_{50} = 0.099 μM), it was found that hydroxymethyl group was important for binding interaction, and the introduced chiral methyl group to compound **11** further increased the activity about 3-fold (compound **12**, IC_{50} = 0.036 μM). This was suggesting that the hydroxymethyl might act as a H-bond donor to the residues of BACE1 and the chiral methyl might have some effects on the conformation orientation.

It was reported that optimization at C-terminus could improve the enzymatic selectivity [20]. Since the catalytic domain of BACE1 was similar to that of other known aspartyl proteases, we selected cathepsin D as a representative to investigate the selectivity of these BACE1 inhibitors. Herein, in parallel all the triazole derivatives were screened for human cathepsin D. Encouragingly, we found all triazole derivatives inhibited cathepsin D with IC_{50} values above 10 μM, suggesting that optimization at C-terminus indeed improves the enzymatic selectivity as expected.

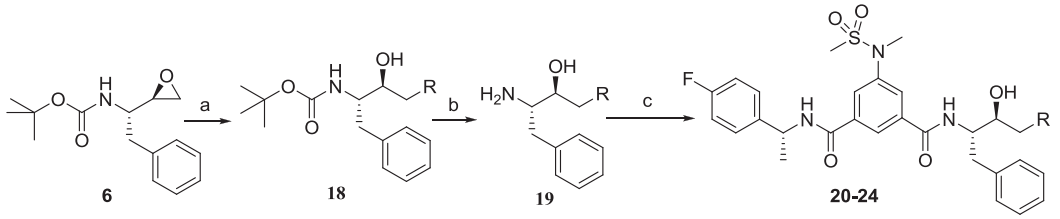

Scheme 3. Synthesis of compound **20**–**24**. Reagents and conditions: (a) K_2CO_3, DMF 100 °C 1 h; (b) TFA/DCM = 1/4; (c) EDCI, HOBt, DIPEA, DMF, r.t. overnight.

Table 2
BACE1 inhibitory activities of triazole isosteres (**20**–**24**).

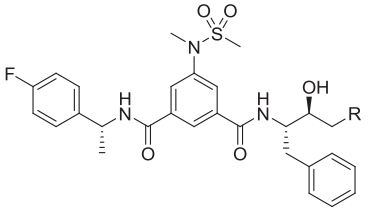

Comp.	R	BACE1 IC_{50}[a] (μM)
10		1.800 ± 0.105
20		0.490 ± 0.033
21		5.900 ± 0.210
22		0.910 ± 0.027
23		4.310 ± 0.134
24		2.100 ± 0.078
OM99-2	/	0.071 ± 0.005

[a] IC_{50} values are means of at least three separate experiments.

2.3. X-ray crystal structure of triazole derivative *12* bound to BACE1

To characterize the binding mode of triazole BACE1 inhibitors, compound **12** was co-crystallized with human BACE1 providing an X-ray crystal structure determined to 1.7 Å resolution (Fig. 3). As expected, The P3-phenyl ring occupied a unique position which spanned S3 and S4 subsites and caused a significant positional shift of a protein loop containing residues from 8 to 13 (the 10's loop) located in the S3/S4 pocket. The P2-sulfonamide functionality fitted well into the S2 pocket and made extensive interactions with BACE1. One of the sulfonamide oxygen atoms formed hydrogen bond via a water molecule with the Ser325 hydroxyl oxygen (3.1 Å and 2.6 Å). The same sulfone oxygen also made ionic interactions with the guanidine side chain of Arg235. Another sulfonamide oxygen made hydrogen bonds to Thr232 and Asn233 main chain nitrogen atoms (3.2 Å and 3.0 Å, respectively). While the phenyl group of compound **12** occupied the S1 region of BACE1, the hydroxyl of central core could form effective hydrogen bonds with active site aspartic acid residue Asp228 (2.7 Å) and Asp32 (2.8 Å). The triazole extended to polar S1′ subpocket. And water molecules played important roles in the hydrogen bond network. It was shown that there was not only a direct hydrogen bonding interaction between the N2 atom of 1,2,3-triazole and the side-chain of residue Thr72 (3.3 Å) but also two indirect hydrogen bonds formed between the hydroxymethyl group substituted on triazole and the main-chain of Pro70 via two water molecules. As shown in Table 1, compound **10** which bound only with Thr72 had moderate binding affinity toward BACE1. When we introduced the interactions with Pro70 (compounds **11**, **12**) it led to great effect on inhibitory activity against BACE1. It gave us an implication that both Pro70 and Thr72 located in the flap region were the critical components of the binding pocket. The interactions between the compound **12** and these two residues made the flap adopt the close conformation, which strengthened the binding to BACE1 along with other interactions from the N-terminus and the central core of compound **12**.

2.4. Bioisosterism and pyrazole scaffold

Although triazole inhibitors exhibited high activity toward BACE1 in enzymatic assays, their cellular inhibitory potencies were poor which limited their follow-up studies. Table 1 showed that all

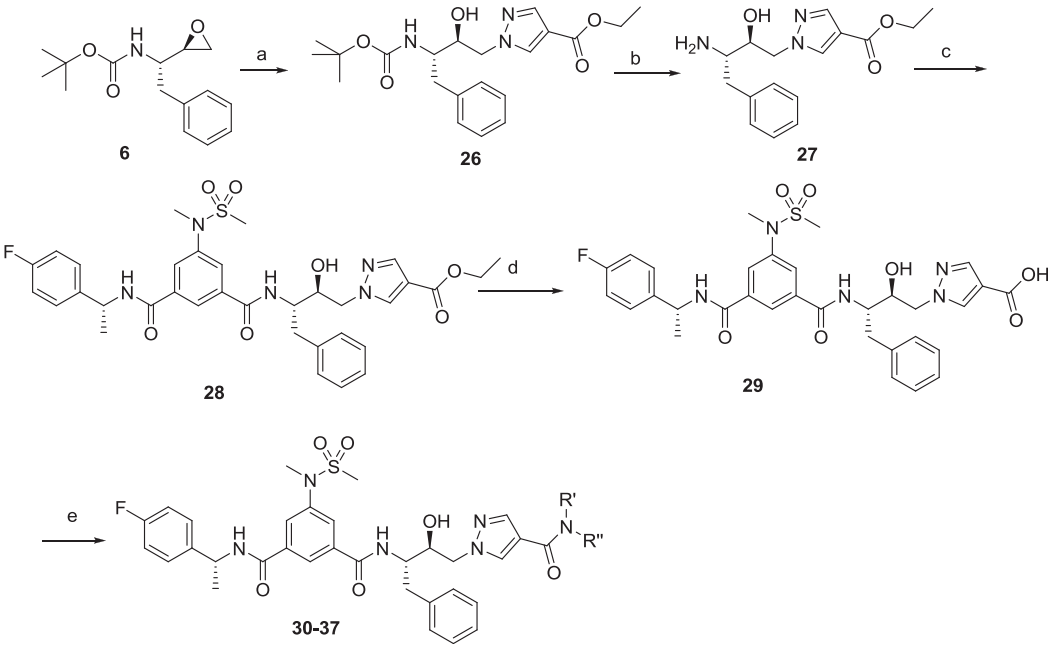

Scheme 4. Synthesis of compound **30**–**37**. Reagents and conditions: (a) K_2CO_3, DMF 100 °C 1 h; (b) TFA/DCM = 1/4; (c) EDCI, HOBt, DIPEA, DMF, MW, r.t. overnight; (d) NaOH, THF/EtOH/H_2O = 2/2/1, reflux 2 h; (e) amine, EDCI, HOBt, DIPEA, DMF, r.t. overnight.

Table 3
BACE1, cathepsin D enzyme data and HEK239 cellular-inhibitory activities of pyrazole derivatives (**28**–**37**).

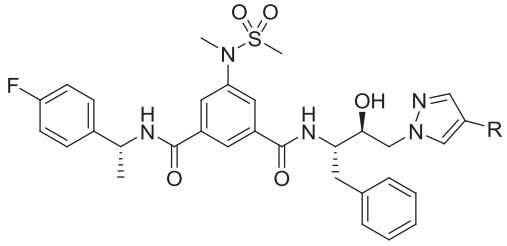

Comp.	R	BACE1 IC_{50} (μM)[a]	CatD-inhibition (%) at 20 μg/mL[b]	CatD IC_{50} (μM)[a]	HEK293 inhibition (10 μM[b])	HEK293 inhibition (1 μM[b])
20	H	0.490 ± 0.033	13.23	>30	7.59	6.35
25		1.210 ± 0.110	−8.08	>30	ND	ND
28	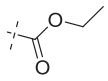	0.051 ± 0.006	22.17	>30	57.01	24.44
30		0.570 ± 0.021	−8.22	>30	56.01	42.59
31		0.256 ± 0.019	−7.97	>30	53.37	40.44
32		0.053 ± 0.005	−6.73	>30	54.78	28.77
33	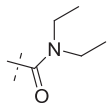	0.230 ± 0.029	−15.08	>30	58.69	46.26
34	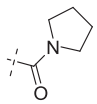	0.074 ± 0.008	−16.78	>30	48.74	29.17
35	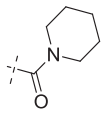	0.076 ± 0.005	−6.72	>30	55.66	25.33
36	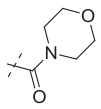	0.027 ± 0.003	9.60	>30	46.58	36.88
37	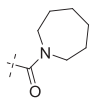	0.025 ± 0.003	−7.42	>30	40.61	32.89
OM99-2	/	0.071 ± 0.005	ND[c]	ND	ND	ND

[a] IC_{50} values are means of at least three separate experiments.
[b] All inhibitory values are means of at least three separate experiments.
[c] 'ND' means the IC_{50} were not determined.

the triazole compounds displayed low inhibitory effects on endogenous BACE1 activity in HEK293 cells transfected with human βAPP695wt (<50% inhibition ratio at 10 μM). In order to improve cellular inhibitory potency, the other five-membered heterocyclic rings were employed to substitute the triazole ring. According to the interaction mode showing in Fig. 3, the N2 atom of triazole is important to hydrogen bond formation. We selected some five-membered heterocycles instead of the triazole scaffold, such as pyrazole, 1,2,4-triazole, the (1*H*)-tetrazole and the (2*H*)-tetrazole for preliminary SAR study. We also prepared the imidazole analog for examining the importance of this specified nitrogen in five-membered heterocycle. The inhibitory activities of these isosteres against BACE1 were summarized in Table 2.

As shown in Table 2, compounds bearing different triazole isosteres at C-terminus showed diverse inhibitory potencies against BACE1. As expected, pyrazole **20** (IC_{50} = 0.490 μM) and 1,2,4-triazole **22** (IC_{50} = 0.910 μM), exhibited higher potency than the initial triazole compound **10** (IC_{50} = 1.800 μM). Analyzing the X-ray

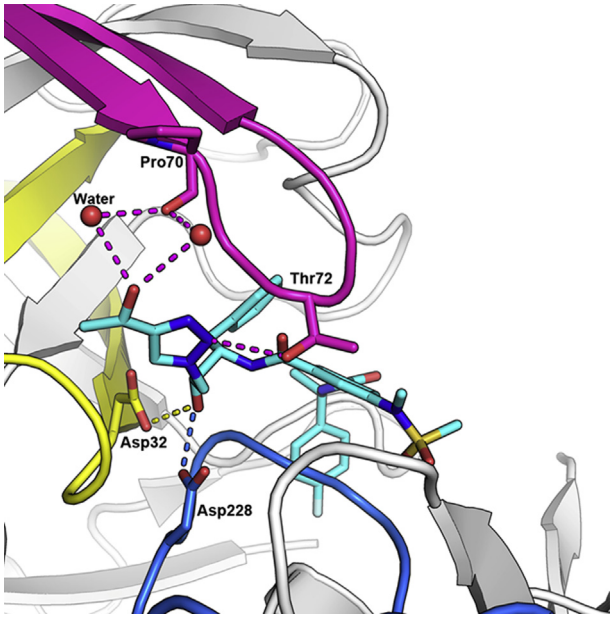

Fig. 3. The crystal structures of BACE1 in complex with compound **12** (PDB ID code: 3UQX).

crystal structure of BACE1 in complex with compound **12** and compound **20**, we found pyrazole and triazole could overlap perfectly, and pyrazole fitted at the entrance of C-terminus. There was a direct hydrogen binding interaction between the N2 atom of pyrazole and Thr72 (3.1 Å) as well. The other three isosteres (compounds **21**, **23**, **24**) displayed weak potencies against BACE1. Compound **21** bearing imidazole group could not form a hydrogen bond with Thr72, which led to a dramatically decrease of inhibitory activity, and the IC_{50} value was dropped to 5.9 μM. This result confirmed the importance of the hydrogen bond between the N2 atom of pyrazole and Thr72. The inhibitory potencies of two tetrazole analogs (**23**, **24**) decreased. This might be due to some changes in their physicochemical property. Given to the drug-likeness and potencies of these five isosteres, we chose pyrazole as a functional group at the entrance of the C-terminus of the inhibitor for further SAR study.

2.5. Biological data and SAR of pyrazole derivatives

Structural analysis revealed that there were still two water molecules in the place of two water molecules in triazole's conformation in the polar S1′–S2′ subpocket (Fig. 4A). As we all know that water molecules could act as not only hydrogen donor but also hydrogen acceptor. In the view of the above analysis, the ester and amide aroused our great interest to be considered as substituent to the pyrazole scaffold. Their carboxyl oxygen atoms might act as hydrogen acceptor through water molecule binding with Pro70, which was expected to strengthen the inhibitory potency. Subsequently 4-ester and 4-amide substituted pyrazole derivatives were designed and investigated the BACE1 and cathepsin D inhibitory activities. The structure–activity relationship (SAR) of 4-substitued pyrazoles was summarized in Table 3.

As we expected, the 4-substituted carbethoxyl compound **28** (IC_{50} = 0.051 μM) had nearly ten-fold potency than that of the compound **20**, suggesting that the carbethoxyl might act as a hydrogen acceptor to form direct or indirect hydrogen bonding interactions with Pro70 in the active site of BACE1. Fortunately an X-ray crystal structure of BACE1 in complex with compound **28** was obtained and the interaction mode was illustrated in Fig. 4B. The carboxyl oxygen of compound **28** formed one water-mediated hydrogen bond with the residue Pro70 (3.4 Å and 2.9 Å) in addition to the direct hydrogen bond that was formed between the N2 atom of pyrazole ring and the residue Thr72 (3.3 Å). These results were in agreement with our previous speculation, and this might be the reason that the inhibitory potencies were greatly strengthened. It was most likely that the amide analogs bound with enzyme in a conformation similar to compound **28**. Clearly, cycle amides (compounds **34**–**37**) were more potent than chain amides (**31**, **33**) (Table 3). The suberyl amide compound **37** (IC_{50} = 0.025 μM) had nearly 3-fold more potent than that of OM99-2 (IC_{50} = 0.071 μM). Meanwhile, all the pyrazole derivatives showed low inhibitory activities toward cathepsin D and the inhibition ratios were all below

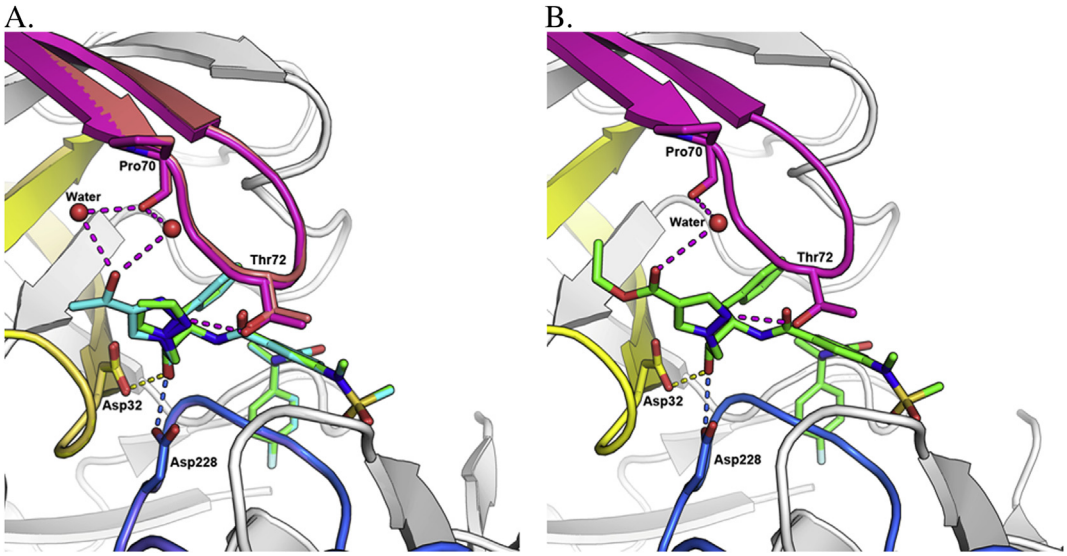

Fig. 4. A. Superposition of the crystal structures of BACE1 in complex with compound **12** (green) and **20** (magenta) (PDB ID code: 3UQX, 3UQU). The position of the two compounds was overlapped well. B. The crystal structures of BACE1 in complex with compound **28** (PDB ID code: 3UQW). The compounds were shown in sticks and two residues, Thr72 and Pro70, were displayed with line. The dash lines represented the hydrogen bonds. (For interpretation of the references to color in this figure legend, the reader is referred to the web version of this article.)

50% at 20 μg/mL. To our surprise, the potency of compound **25** (IC_{50} = 1.210 μM) with hydroxymethyl substituted at 4-position, decreased dramatically comparing with its triazole analog **11** (IC_{50} = 0.099 μM). Therefore, we didn't further optimize pyrazole analogs with hydroxy group, and paid our attention to pyrazole analogs with carbonyl group.

According to intriguing findings described above, all the pyrazole analogs were selected to examine the cellular inhibition of endogenous BACE1 activity in HEK293 cells transfected with human βAPP695wt. The percentage of whole cell Aβ reduction (sandwich Elisa) was used to monitor inhibitory effects of the compounds. The results showed that all compounds displayed moderate inhibitory effects on the cell-based assay at 1 μM, which demonstrated that pyrazole acting as C-terminus scaffold were better than triazole analogs according to the cellular activities (Table 3). Among these, compounds **30** and **33** exhibited good inhibition effects on Aβ production in the cell-based assay. Although that cycle amides were more potent than chain amides toward BACE1 in enzymatic assay, while, chain amides were better than cycle amides in cellular assay. This might be due to the better permeability of the chain amides than the cycle amides. In recent years, there have been reported many BACE1 inhibitors with better drug-like properties [10], such as lower molecular weight, higher bioavailability, the better BBB penetration. We are aware that our compounds have undesirable drug-like properties. But in the present work, the aim is to explore the novel scaffold binding to S1′ subpocket. The pyrazole was found that is a good functional group as C-terminus scaffold, which can contribute to the design of new inhibitors by incorporating the pyrazole ring. However, further studies will be needed to test the adaptability of this scaffold.

3. Conclusion

Toward the goal to obtain novel C-terminus groups for BACE1 inhibitors, we utilized the click chemistry and *in situ* screening approach to design and investigate triazole derivatives on the basis of the previous study of our group. Among these triazole derivatives, compound **12** (IC_{50} = 0.036 μM) exhibited better enzyme-inhibiting potency, comparable to that of OM99-2 (IC_{50} = 0.071 μM). With the aid of the crystal structure of BACE1 in complex with compound **12**, we found that Pro70 and Thr72 which located in the flap region were the critical components for interaction with substituted triazole group. On the basis of structural analysis and bioisosterism, pyrazole derivatives were prepared to extend the SAR of this class of molecules and improve the cellular activities. As a result, pyrazole derivatives, which maintained potent BACE1 activities in enzymatic assay and good selectivity over cathepsin D, showed improvement of cellular activities, especially compound **30** and **33**. From the present work, the pyrazole scaffold could be considered as better C-terminus of BACE1 inhibitors comparing that of triazole. And Pro70 and Thr72 might be taken as promising subsite for developing selective BACE1 inhibitors as anti-AD drugs.

4. Experimental section

4.1. General methods

The ^{1}H NMR (300 MHz or 400 MHz) spectra were recorded on Varian Mercury-300 or 400 High Performance Digital FT-NMR using tetramethylsilane as an internal standard and the ^{13}C NMR (100 MHz) spectra were determined with Varian Mercury-400 High Performance Digital FT-NMR. The LC–MS were carried out on Thermo Finnigan LCQDECAXP and HRMS were performed with Finnigan MAT 95, EI: 70 eV, *R*: 10,000. The purity of the stereospecifical target compounds was recorded on HPLC system (HP 1100series, Agilent Technologies, Palo Alto, USA) by two different gradient methods using an YMC ODS column (50 × 4.6 mm, 5 μm particle size). The optical rotation value was determined with PerkinElmer-341 (589 nm). All reagents are of analytical grade pure and used without further purification.

4.1.1. *tert*-Butyl (2*S*,3*S*)-4-azido-3-hydroxy-1-phenylbutan-2-ylcarbamate (**7**)

To a solution of compound **6** (770 mg, 2.93 mmol) in methanol (20 mL) was added NH_4Cl (282 mg, 5.27 mmol), NaN_3 (457 mg, 7.03 mmol). The mixture was heated to reflux overnight. and then the solvent was concentrated under reduced pressure. Water (30 mL) was added into the reaction. The solution was extracted with EtOAc twice (30 mL × 2) and the combined organic layers were washed by diluted HCl, saturated $NaHCO_3$, saturated brine twice (15 mL × 2) by turns. Then the organic layers were dried over Na_2SO_4, filtered and evaporated to give the residue, which was purified by silica gel chromatography to afford **7** (810 mg, 90.3%). ^{1}H NMR (300 MHz, $CDCl_3$): δ 7.29–7.27 (m, 5H), 4.60 (d, *J* = 8.4 Hz, 1H), 3.82–3.78 (m, 2H), 3.42–3.37 (m, 3H), 2.90–2.93 (m, 2H), 1.37 (s, 9H); ^{13}C NMR (100 MHz, $CDCl_3$): δ 156.1, 137.8, 129.4, 128.5, 126.3, 79.8, 72.1, 55.1, 53.8, 38.2, 28.2; LCMS (ESI): 306.7 $[M + H]^+$; HRMS: calcd for $C_{15}H_{22}N_4O_3Na$ 329.1590, found $C_{15}H_{22}N_4O_3Na$ 329.1602; $[\alpha]_D^{19} = -51.5^\circ$ (*c* 1.000, MeOH).

4.1.2. N^1-((2*S*,3*S*)-4-Azido-3-hydroxy-1-phenylbutan-2-yl)-N^3-((*R*)-1-(4-fluorophenyl)ethyl)-5-(*N*-methylmethylsulfonamido) isophthalamide (**9**)

To a solution of CF_3COOH (1 mL) in CH_2Cl_2 (4 mL) was added **7** (92 mg, 0.3 mmol). The mixture was at room temperature for 3 h, and then it was concentrated under reduced pressure to afford the crude product **8** used without further purification. To a solution of the product (92 mg, 0.3 mmol) in DMF (8 mL) was added 3-[(*R*)-1-(4-fluorophenyl)ethylaminocarbonyl]-5-[methyl(methylsulfonyl) amino]benzoic acid (106 mg, 0.27 mmol), EDCI (52 mg, 0.27 mmol), HOBt (37 mg, 0.27 mmol), DIPEA (99 μL, 0.6 mmol) was added and the mixture was allowed to react overnight at room temperature. Then the resulting mixture was diluted by 50 mL EtOAc and washed with dilute HCl aqueous solution twice (30 mL × 2), saturated aqueous $NaHCO_3$ twice (30 mL × 2) and saturated brine once (30 mL) sequentially. The organic layers were dried over Na_2SO_4, filtered and evaporated to give the residue, which was purified by silica gel chromatography to afford **9** (170 mg, 97.4%). ^{1}H NMR (300 MHz, CD_3OD): δ 8.08 (s, 1H), 7.98 (t, *J* = 1.5 Hz, 1H), 7.86 (t, *J* = 1.2 Hz, 1H), 7.42 (m, 2H), 7.27 (m, 4H), 7.16 (m, 1H), 7.06 (m, 2H), 5.22 (m, 1H), 4.40 (m, 1H), 3.85 (m, 1H), 3.32 (m, 5H), 2.96–3.06 (m, 2H), 2.95 (s, 3H), 1.57–1.52 (d, *J* = 6.9 Hz, 3H); ^{13}C NMR (100 MHz, $CDCl_3$): δ 165.9, 164.8, 161.9 (d, *J* = 245 Hz, 1C), 142.1, 138.5, 137.3, 135.6, 135.4, 129.2, 128.7, 127.9, 127.8, 127.7, 127.6, 126.8, 124.1, 70.4, 54.8, 53.6, 49.2, 37.9, 37.8, 35.5, 21.6; LCMS (ESI): 583.0 $[M + H]^+$; HRMS: calcd for $C_{28}H_{31}N_6O_5FSNa$ 605.1958, found $C_{28}H_{31}N_6O_5FSNa$ 605.1964; $[\alpha]_D^{20} = -79.2^\circ$ (*c* 0.5, MeOH).

4.2. General method for preparation of compounds **10**–**17** (exemplified by **10**)

4.2.1. N^1-((*R*)-1-(4-Fluorophenyl)ethyl)-N^3-((2*S*,3*S*)-3-hydroxy-1-phenyl-4-(1*H*-1,2,3-triazol-1-yl)butan-2-yl)-5-(*N*-methylmethylsulfonamido)isophthalamide (**10**)

To a solution of compound **9** (29 mg, 0.05 mmol) in THF (0.8 mL) and H_2O (0.2 mL), was added ethynyltrimethylsilane (28 μL, 0.2 mmol), followed by addition of sodium ascorbate (2 mg, 0.01 mmol) and CuI (1 mg, 0.005 mmol). This reaction was heated at 50 °C for 12 h. The reaction mixture was concentrated under reduced pressure to afford the crude product used without further

purification. The remaining solid was dissolved in THF (1 mL). Tetrabutylammonium fluoride (52 mg, 0.2 mmol) was added and the mixture was allowed to react overnight at room temperature. The mixture was filtered and evaporated to give the residue, which was purified by silica gel chromatography to afford **10** (21 mg, 70.0%). ^{1}H NMR (300 MHz, CD_3OD): δ 8.14 (m, 1H), 8.00 (s, 2H), 7.89 (s, 1H), 7.70 (s, 1H), 7.42–7.40 (m, 2H), 7.30–7.21 (m, 4H), 7.17–7.14 (m, 1H), 7.08–7.05 (t, J = 8.7 Hz, 2H), 5.25–5.19 (q, J = 7.0 Hz, 1H), 4.63–4.57 (m, 1H), 4.50–4.37 (m, 2H), 4.19–4.16 (m, 1H), 3.34 (s, 3H), 3.13–2.99 (m, 2H), 2.95 (s, 3H), 1.57–1.52 (d, J = 7.0 Hz, 3H); ^{13}C NMR (100 MHz, $CDCl_3$): δ 166.03, 164.82, 162.80 (d, J = 245 Hz, 1C), 141.88, 139.64, 137.74, 137.58, 135.46, 135.11, 133.14, 129.22, 128.14, 127.91, 126.36, 125.33, 124.08, 115.13, 115.07, 70.67, 58.58, 54.31, 53.95, 49.27, 37.74, 35.33, 23.63; LCMS (ESI): 609.1 $[M + H]^+$; HRMS: calcd for $C_{30}H_{33}FN_6O_5SNa$ 631.2115, found $C_{30}H_{33}FN_6O_5SNa$ 631.2114; $[\alpha]_D^{17} = -34.0^\circ$ (c 0.35, MeOH).

4.2.2. N^1-((R)-1-(4-Fluorophenyl)ethyl)-N^3-((2S,3S)-3-hydroxy-4-(4-(hydroxylmethyl)-1H-1,2,3-triazol-1-yl)-1-phenylbutan-2-yl)-5-(N-methylmethylsulfonamido)isophthalamide (**11**)

To a solution of compound **9** (29 mg, 0.05 mmol) in THF (0.8 mL) and H_2O (0.2 mL), was added prop-2-yn-1-ol (12 μL, 0.2 mmol), followed by addition of sodium ascorbate (2 mg, 0.01 mmol) and CuI (1 mg, 0.005 mmol). This reaction was heated at 50 °C for 12 h. The reaction mixture was concentrated under reduced pressure to afford the crude product, which was purified by silica gel chromatography to afford **11** (23 mg, 70.1%). ^{1}H NMR (300 MHz, CD_3OD): δ 8.12 (s, 1H), 7.99–7.98 (m, 1H), 7.94 (s, 1H), 7.89–7.88 (m, 1H), 7.43–7.40 (m, 2H), 7.30–7.21 (m, 4H), 7.17–7.14 (m, 1H), 7.09–7.03 (t, J = 9.0 Hz, 2H), 5.27–5.20 (q, J = 7.0 Hz, 1H), 4.66 (s, 2H), 4.59–4.53 (m, 1H), 4.49–4.45 (m, 1H), 4.41–4.33 (m, 1H), 4.17–4.15 (m, 1H), 3.35 (s, 3H), 3.12–2.99 (m, 2H), 2.96 (s, 3H), 1.58–1.54 (d, J = 7.0 Hz, 3H); ^{13}C NMR (100 MHz, $CDCl_3$): δ 166.6, 164.9, 160.5 (d, J = 245 Hz, 1C), 141.7, 139.0, 137.7, 137.4, 135.7, 135.0, 133.1, 129.1, 128.4, 127.6, 126.5, 124.7, 123.9, 115.3, 115.0, 70.9, 55.4, 54.2, 53.6, 48.8, 37.6, 37.3, 35.5, 21.6; LCMS (ESI): 639.1 $[M + H]^+$; HRMS: calcd for $C_{31}H_{35}N_6O_5FSNa$ 661.2221, found $C_{31}H_{35}N_6O_5FSNa$ 661.2231; $[\alpha]_D^{15} = -107^\circ$ (c 0.15, MeOH).

4.2.3. N^1-((R)-1-(4-Fluorophenyl)ethyl)-N^3-((2S,3S)-3-hydroxy-4-(4-((R)-1-hydroxy ethyl)-1H-1,2,3-triazol-1-yl)-1-phenylbutan-2-yl)-5-(N-methylmethylsulfonamido) isophthalamide (**12**)

Compound **12** was obtained from **9** and (*R*)-but-3-yn-2-ol (16 μL, 0.2 mmol) according to the similar procedure used to prepare **11**. The crude product was purified by silica gel chromatography to afford **12** (21 mg, 62.7%). ^{1}H NMR (300 MHz, CD_3OD): δ 8.12 (s, 1H), 7.99 (s, 1H), 7.89 (s, 2H), 7.44–7.40 (m, 2H), 7.27–7.23 (m, 4H), 7.17–7.16 (m, 1H), 7.12–7.04 (m, 2H), 5.27–5.20 (q, J = 7.0 Hz, 1H), 4.96–4.94 (m, 1H), 4.57–4.51 (m, 1H), 4.49–4.42 (m, 1H), 4.40–4.32 (m, 1H), 4.17–4.15 (m, 1H), 3.35 (s, 3H), 3.12–2.97 (m, 2H), 2.96 (s, 3H), 1.58–1.56 (d, J = 7.0 Hz, 3H), 1.51–1.49 (d, J = 6.6 Hz, 3H); ^{13}C NMR (100 MHz, $CDCl_3$): δ 166.6, 165.1, 161.8 (d, J = 245 Hz, 1C), 141.9, 138.9, 137.5, 137.4, 135.9, 135.1, 129.2, 128.7, 128.0, 127.9, 126.8, 124.2, 122.7, 115.4, 115.2, 72.1, 62.4, 54.6, 53.2, 49.1, 37.8, 35.8, 35.7, 22.8, 21.6; LCMS (ESI): 653.1 $[M + H]^+$; HRMS: calcd for $C_{32}H_{37}FN_6O_6SNa$ 675.2377, found $C_{32}H_{37}FN_6O_6SNa$ 675.2390; $[\alpha]_D^{23} = -36^\circ$ (c 0.20, MeOH).

4.2.4. N^1-((R)-1-(4-Fluorophenyl)ethyl)-N^3-((2S,3S)-3-hydroxy-1-phenyl-4-(4-phenyl-1H-1,2,3-triazol-1-yl)butan-2-yl)-5-(N-methylmethylsulfonamido)isophthalamide (**13**)

Compound **13** was obtained from **9** and ethynylbenzene (22 μL, 0.2 mmol) according to the similar procedure used to prepare **11**. The crude product was purified by silica gel chromatography to afford **13** (31 mg, 91.5%). ^{1}H NMR (300 MHz, CD_3OD): δ 8.30–8.29 (m, 1H), 8.14–8.12 (m, 1H), 7.98–7.97 (m, 1H), 7.89–7.88 (m, 1H), 7.77–7.74 (m, 2H), 7.44–7.37 (m, 4H), 7.33–7.21 (m, 5H), 7.15–7.12 (m, 1H), 7.09–7.04 (m, 2H), 5.26–5.19 (q, J = 6.7 Hz, 1H), 4.63–4.57 (m, 1H), 4.53–4.39 (m, 2H), 4.21–4.19 (m, 1H), 3.34 (s, 3H), 3.12–2.99 (m, 2H), 2.94 (s, 3H), 1.57–1.54 (d, J = 6.7 Hz, 3H); ^{13}C NMR (100 MHz, $CDCl_3$): δ 166.2, 164.8, 161.9 (d, J = 245 Hz, 1C), 147.3, 142.1, 138.7, 137.4, 135.8, 135.3, 129.7, 129.3, 128.8, 128.7, 128.3, 128.0, 127.9, 126.8, 125.4, 124.0, 121.4, 115.6, 115.4, 70.4, 54.7, 54.1, 49.2, 38.0, 37.9, 35.6, 21.7; LCMS (ESI): 685.2 $[M + H]^+$; HRMS: calcd for $C_{36}H_{37}N_6O_5FSNa$ 707.2428, found $C_{36}H_{37}N_6O_5FSNa$ 707.2393; $[\alpha]_D^{17} = -60.7^\circ$ (c 0.95, MeOH).

4.2.5. N^1-((R)-1-(4-Fluorophenyl)ethyl)-N^3-((2S,3S)-3-hydroxy-4-(4-(4-methoxyphenyl)-1H-1,2,3-triazol-1-yl)-1-phenylbutan-2-yl)-5-(N-methylmethylsulfonamido)isophthalamide (**14**)

Compound **14** was obtained from **9** and 1-ethynyl-4-methoxybenzene (26 μL, 0.2 mmol) according to the similar procedure used to prepare **11**. The crude product was purified by silica gel chromatography to afford **14** (30 mg, 82.1%). ^{1}H NMR (300 MHz, CD_3OD): δ 8.19 (s, 1H), 8.12 (s, 1H), 7.98–7.97 (m, 1H), 7.89–7.87 (m, 1H), 7.68–7.65 (m, 2H), 7.46–7.40 (m, 2H), 7.31–7.21 (m, 4H), 7.18–7.12 (m, 1H), 7.08–7.03 (m, 2H), 6.97–6.94 (m, 2H), 5.26–5.20 (q, J = 7.0 Hz, 1H), 4.63–4.57 (m, 1H), 4.52–4.45 (m, 1H), 4.42–4.39 (m, 1H), 4.24–4.21 (m, 1H), 3.81 (s, 3H), 3.33 (s, 3H), 2.97–3.15 (m, 2H), 2.95 (s, 3H), 1.58–1.54 (d, J = 7.0 Hz, 3H); ^{13}C NMR (100 MHz, $CDCl_3$): δ 166.1, 164.6, 163.1 (d, J = 245 Hz, 1C), 160.6, 159.5, 147.0, 142.1, 138.4, 137.1, 135.7, 135.0, 129.5, 128.4, 127.7, 127.6, 126.7, 123.9, 122.4120.6, 115.6, 115.1, 114.1, 70.5, 55.1, 54.5, 53.8, 49.1, 38.0, 37.8, 35.4, 21.6; LCMS (ESI): 715.1 $[M + H]^+$; HRMS: calcd for $C_{37}H_{39}N_6O_6FSNa$ 737.2534, found $C_{37}H_{39}N_6O_6FSNa$ 737.2514; $[\alpha]_D^{18} = -52.6^\circ$ (c 1.10, MeOH).

4.2.6. N^1-((2S,3S)-4-(4-Cyclohexyl-1H-1,2,3-triazol-1-yl)-3-hydroxy-1-phenylbutan-2-yl)-N^3-((R)-1-(4-fluorophenyl)ethyl)-5-(N-methylmethylsulfonamido)isophthalamide (**15**)

Compound **15** was obtained from **9** and ethynylcyclohexane (26 μL, 0.2 mmol) according to the similar procedure used to prepare **11**. The crude product was purified by silica gel chromatography to afford **15** (29 mg, 82.1%). ^{1}H NMR (300 MHz, CD_3OD): δ 8.12 (s, 1H), 8.00 (s, 1H), 7.89 (s, 1H), 7.72 (s, 1H), 7.45–7.40 (m, 2H), 7.29–7.21 (m, 4H), 7.17–7.14 (m, 1H), 7.08–7.03 (t, J = 8.7 Hz, 2H), 5.26–5.22 (q, J = 7.0 Hz, 1H), 4.54–4.40 (m, 2H), 4.37–4.30 (m, 1H), 4.17–4.14 (m, 1H), 3.35 (s, 3H), 3.11–2.98 (m, 2H), 2.96 (s, 3H), 2.69–2.65 (m, 1H), 1.99–1.96 (m, 2H), 1.80–1.70 (m, 3H), 1.59–1.57 (d, J = 7.0 Hz, 3H), 1.45–1.25 (m, 5H); ^{13}C NMR (100 MHz, $CDCl_3$): δ 166.0, 164.7, 163.2 (d, J = 245 Hz, 1C), 153.2, 142.2, 138.6, 138.1, 137.3, 135.8, 135.2, 129.1, 128.2, 127.7, 126.7, 123.8, 121.1, 115.5, 115.1, 70.1, 58.5, 54.3, 53.9, 49.0, 37.9, 37.6, 35.4, 34.8, 32.6, 25.8, 21.7; LCMS (ESI): 691.2 $[M + H]^+$; HRMS: calcd for $C_{36}H_{43}N_6O_5FSNa$ 713.2897, found $C_{36}H_{43}N_6O_5FSNa$ 713.2898; $[\alpha]_D^{17} = -86^\circ$ (c 0.30, MeOH).

4.2.7. N^1-((R)-1-(4-Fluorophenyl)ethyl)-N^3-((2S,3S)-3-hydroxy-4-(5-(hydroxymethyl)-1H-1,2,3-triazol-1-yl)-1-phenylbutan-2-yl)-5-(N-methylmethylsulfonamido)isophthalamide (**16**)

To a solution of compound **9** (29 mg, 0.05 mmol) in THF (1.0 mL) prop-2-yn-1-ol (12 μL, 0.2 mmol) was added, followed by addition of Cp*Ru $(PPh_3)_3Cl_2$ (4 mg, 0.005 mmol). This reaction was heated to reflux under argon for 8 h. The resulting mixture was concentrated under reduced pressure to afford the crude product, which was purified by silica gel chromatography to afford **16** (17 mg, 51.1%). ^{1}H NMR (300 MHz, CD_3OD): δ 8.12 (s, 1H), 7.99 (s, 1H), 7.88 (s, 1H), 7.63 (s, 1H), 7.45–7.40 (m, 2H), 7.32–7.22 (m, 4H), 7.17–7.14 (m, 1H), 7.09–7.03 (t, J = 8.7 Hz, 2H), 5.27–5.20 (q, J = 7.1 Hz, 1H), 4.73–4.62 (m, 2H), 4.64–4.57 (m, 1H), 4.53–4.42

(m, 2H), 4.27–4.23 (m, 1H), 3.36 (s, 3H), 3.14–2.99 (m, 2H), 2.96 (s, 3H), 1.59–1.56 (d, J = 7.1 Hz, 3H); ^{13}C NMR (100 MHz, $CDCl_3$): δ 166.26, 164.59, 161.06 (d, J = 245 Hz, 1C), 142.08, 138.71, 137.41, 135.79, 135.37, 129.32, 128.59, 127.80, 127.69, 126.64, 123.89, 115.78, 115.04, 70.20, 69.47, 65.9, 53.72, 51.10, 49.23, 37.97, 35.50, 29.63, 29.00, 21.81; LCMS (ESI): 639.1 $[M + H]^+$; HRMS: calcd for $C_{31}H_{35}N_6O_6FSNa$ 661.2221, found $C_{31}H_{35}N_6O_6FSNa$ 661.2213; $[\alpha]_D^{17} = -58.0^\circ$ (*c* 0.20, MeOH).

4.2.8. N^1-((R)-1-(4-Fluorophenyl)ethyl)-N^3-((2S,3S)-3-hydroxy-1-phenyl-4-(5-phenyl-1H-1,2,3-triazol-1-yl)butan-2-yl)-5-(N-methylmethylsulfonamido)isophthalamide (**17**)

Compound **17** was obtained from **9** and ethynylbenzene (22 μL, 0.2 mmol) according to the similar procedure used to prepare **16**. The crude product was purified by silica gel chromatography to afford **17** (21 mg, 58.8%). ^{1}H NMR (300 MHz, CD_3OD): δ 8.00–7.98 (m, 2H), 7.78 (s, 1H), 7.74 (s, 1H), 7.48–7.41 (m, 4H), 7.31–7.21 (m, 7H), 7.17–7.12 (m, 1H), 7.09–7.03 (t, J = 8.7 Hz, 2H), 5.28–5.21 (q, J = 7.1 Hz, 1H), 4.49–4.44 (m, 1H), 4.42–4.26 (m, 3H), 3.34 (s, 3H), 3.07–2.96 (m, 2H), 2.95 (s, 3H), 1.58–1.56 (d, J = 7.1 Hz, 3H); ^{13}C NMR (100 MHz, $CDCl_3$): δ 166.1, 164.7, 162.9 (d, J = 245 Hz, 1C), 141.6, 139.2, 138.7, 137.5, 135.8, 135.2, 132.5, 129.6, 129.2, 128.8, 128.3, 128.2, 127.8, 126.7, 126.0, 124.2, 115.7, 115.1, 69.9, 53.8, 51.7, 48.8, 38.1, 37.4, 35.4, 29.6, 21.5; LCMS (ESI): 685.2 $[M + H]^+$; HRMS: calcd for $C_{36}H_{37}N_6O_5FSNa$ 707.2428, found $C_{36}H_{37}N_6O_5FSNa$ 707.2435; $[\alpha]_D^{15} = -90.3^\circ$ (*c* 0.35, MeOH).

4.2.9. N^1-((R)-1-(4-Fluorophenyl)ethyl)-N^3-((2S,3S)-3-hydroxy-1-phenyl-4-(1H-pyrazol-1-yl)butan-2-yl)-5-(N-methylmethylsulfonamido)isophthalamide (**20**)

To a solution of compound **6** (131 mg, 0.50 mmol) in DMF (2 mL) was added pyrazole (51 mg, 0.75 mmol), K_2CO_3 (138 mg, 1.00 mmol). The mixture was heated at 100 °C for 1 h. Reaction mixture was cooled, ice cold water (30 mL) was added and then extracted with EtOAc twice (30 mL × 2) and the combined organic layers were washed by saturated brine (30 mL). Then the organic layers were dried over Na_2SO_4, filtered and evaporated to afford the crude product used without further purification, To a solution of CF_3COOH (1 mL) in CH_2Cl_2 (4 mL) was added the remaining solid (92 mg, 0.30 mmol). The mixture was at room temperature for 3 h, and then it was concentrated under reduced pressure to afford the crude product **19** used without further purification. To a solution of the product (99 mg, 0.30 mmol) in DMF (8 mL) was added 3-[(*R*)-1-(4-fluorophenyl)ethylaminocarbonyl]-5-[methyl (methylsulfonyl)amino]benzoic acid (106 mg, 0.27 mmol), EDCI (52 mg, 0.27 mmol), HOBt (37 mg, 0.27 mmol), DIPEA (99 μL, 0.60 mmol) was added and the mixture was allowed to react overnight at room temperature. Then the resulting mixture was diluted by 50 mL EtOAc and washed with dilute HCl aqueous solution (30 mL), saturated aqueous $NaHCO_3$ (30 mL) and saturated brine (30 mL) sequentially. The organic layers were dried over Na_2SO_4 and evaporated to give the residue, which was purified by silica gel chromatography to afford **20** (149 mg, 91.3%). ^{1}H NMR (300 MHz, CD_3OD): δ 8.12 (s, 1H), 7.99 (s, 1H), 7.89 (s, 1H), 7.63 (s, 1H), 7.46–7.39 (m, 3H), 7.26–7.19 (m, 4H), 7.16–7.13 (m, 1H), 7.08–7.02 (t, J = 8.4 Hz, 2H), 6.24 (s, 1H), 5.24–5.22 (q, J = 6.9 Hz, 1H), 4.41–4.36 (m, 1H), 4.29–4.23 (m, 1H), 4.15–4.10 (m, 2H), 3.34 (s, 3H), 3.08–2.93 (m, 2H), 2.94 (s, 3H), 1.58–1.55 (d, J = 6.9 Hz, 3H); ^{13}C NMR (100 MHz, $CDCl_3$) δ 165.60, 164.47, 163.21 (d, J = 245 Hz, 1C), 142.28, 139.82, 138.44, 137.19, 135.83, 135.45, 130.34, 129.35, 128.65, 127.89, 127.27, 126.48, 123.55, 115.62, 115.19, 105.70, 70.40, 53.46, 49.01, 38.19, 37.51, 35.36, 29.48, 21.51; LCMS (ESI): 608.1 $[M + H]^+$; HRMS: calcd for $C_{31}H_{35}N_5O_5FS$ 608.2343, found $C_{31}H_{35}N_5O_5FS$ 608.2322; $[\alpha]_D^{15} = -42.2^\circ$ (*c* 0.09, MeOH).

4.2.10. N^1-((R)-1-(4-Fluorophenyl)ethyl)-N^3-((2S,3S)-3-hydroxy-4-(1H-imidazol-1-yl)-1-phenylbutan-2-yl)-5-(N-methylmethylsulfonamido)isophthalamide (**21**)

Compound **21** was obtained from **6** and imidazole (51 mg, 0.75 mmol) according to the similar procedure used to prepare **20**. The crude product was purified by silica gel chromatography to afford **21** (141 mg, 88.7%). ^{1}H NMR (300 MHz, CD_3OD): δ 8.10 (s, 1H), 7.99 (s, 1H), 7.89 (s, 1H), 7.44–7.39 (m, 2H), 7.28–7.20 (m, 5H), 7.17–7.14 (m, 2H), 7.08–7.03 (m, 3H), 5.24–5.22 (q, J = 6.6 Hz, 1H), 4.48–4.44 (m, 1H), 4.21–4.18 (m, 1H), 4.00–3.97 (m, 2H), 3.34 (s, 3H), 3.03–2.99 (m, 2H), 2.94 (s, 3H), 1.58–1.55 (d, J = 6.6 Hz, 3H); ^{13}C NMR (100 MHz, $CDCl_3$) δ 166.05, 164.78, 162.91 (d, J = 245 Hz, 1C), 142.35, 139.91, 138.95, 137.55, 135.67, 135.19, 131.22, 129.36, 128.76, 128.24, 128.11, 126.87, 123.87, 115.54, 115.24, 112.40, 70.07, 54.12, 49.28, 38.18, 37.84, 35.86, 31.83, 22.54; LCMS (ESI): 608.3 $[M + H]^+$; HRMS: calcd for $C_{31}H_{35}N_5O_5FS$ 608.2343, found $C_{31}H_{35}N_5O_5FS$ 608.2315; $[\alpha]_D^{15} = -32.5^\circ$ (*c* 0.04, $CHCl_3$).

4.2.11. N^1-((R)-1-(4-Fluorophenyl)ethyl)-N^3-((2S,3S)-3-hydroxy-1-phenyl-4-(1H-1,2,4-triazol-1-yl)butan-2-yl)-5-(N-methylmethylsulfonamido)isophthalamide (**22**)

Compound **22** was obtained from **6** and 1,2,4-triazole (52 mg, 0.75 mmol) according to the similar procedure used to prepare **20**. The crude product was purified by silica gel chromatography to afford **22** (137 mg, 86.2%). ^{1}H NMR (300 MHz, CD_3OD): δ 8.21 (s, 1H), 8.12 (s, 1H), 7.99 (s, 1H), 7.95 (s, 1H), 7.89 (s, 1H), 7.44–7.40 (m, 2H), 7.28–7.21 (m, 4H), 7.17–7.12 (m, 1H), 7.08–7.03 (t, J = 8.7 Hz, 2H), 5.24–5.22 (q, J = 7.2 Hz, 1H), 4.45–4.40 (m, 1H), 4.37–4.31 (m, 1H), 4.25–4.11 (m, 2H), 3.34 (s, 3H), 3.10–2.95 (m, 2H), 2.97 (s, 3H), 1.58–1.56 (d, J = 7.2 Hz, 3H); ^{13}C NMR (100 MHz, $CDCl_3$): δ 166.08, 164.85, 163.03 (d, J = 245 Hz, 1C), 151.15, 143.97, 141.94, 138.69, 137.35, 135.71, 135.32, 129.15, 128.59, 127.88, 127.80, 126.73, 124.34, 115.43, 115.22, 69.78, 53.80, 53.54, 49.04, 37.86, 37.79, 35.49, 21.56; LCMS (ESI): 609.3 $[M + H]^+$; HRMS: calcd for $C_{30}H_{34}N_6O_5FS$ 609.2295, found $C_{30}H_{34}N_6O_5FS$ 609.2307; $[\alpha]_D^{15} = -251.9^\circ$ (*c* 0.21, $CHCl_3$).

4.2.12. N^1-((R)-1-(4-Fluorophenyl)ethyl)-N^3-((2S,3S)-3-hydroxy-1-phenyl-4-(1H-tetrazol-1-yl)butan-2-yl)-5-(N-methylmethylsulfonamido)isophthalamide (**23**) and N^1-((R)-1-(4-fluorophenyl)ethyl)-N^3-((2S,3S)-3-hydroxy-1-phenyl-4-(2H-tetrazol-2-yl)butan-2-yl)-5-(N-methylmethylsulfonamido)isophthalamide (**24**)

To a solution of compound **6** (131 mg, 0.50 mmol) in DMF (2 mL) was added tetrazole (53 mg, 0.75 mmol), K_2CO_3 (138 mg, 1.00 mmol). The mixture was heated at 100 °C for 1 h. Reaction mixture was cooled, ice cold water (30 mL) was added and then extracted with EtOAc twice (30 mL × 2) and the combined organic layers were washed by saturated brine (30 mL). Then the organic layers were dried over Na_2SO_4, filtered and evaporated to afford the crude product used without further purification, To a solution of CF_3COOH (1 mL) in CH_2Cl_2 (4 mL) was added the remaining solid (92 mg, 0.30 mmol). The mixture was stirred at room temperature for 3 h, and then it was concentrated under reduced pressure to afford the crude product used without further purification. To a solution of the product (100 mg, 0.30 mmol) in DMF (8 mL) was added 3-[(*R*)-1-(4-fluorophenyl)ethylaminocarbonyl]-5-[methyl (methylsulfonyl)amino]benzoic acid (106 mg, 0.27 mmol), EDCI (52 mg, 0.27 mmol), HOBt (37 mg, 0.27 mmol), DIPEA (99 μL, 0.60 mmol) was added and the mixture was allowed to react overnight at room temperature. Then the resulting mixture was diluted by 50 mL EtOAc and washed with dilute HCl aqueous solution (30 mL), saturated aqueous $NaHCO_3$ (30 mL) and saturated brine (30 mL) sequentially. The organic layers were dried over Na_2SO_4, filtered and evaporated to give the residue, which was purified by silica gel chromatography to afford **23** (68 mg, 41.3%)

and **24** (74 mg, 45.4%). ^{1}H NMR (300 MHz, CD_3OD): δ 8.68 (s, 1H), 8.13 (s, 1H), 7.98 (s, 1H), 7.89 (s, 1H), 7.44–7.39 (m, 2H), 7.30–7.21 (m, 4H), 7.17–7.13 (m, 1H), 7.08–7.02 (t, J = 8.7 Hz, 2H), 5.24–5.21 (q, J = 7.5 Hz, 1H), 4.76–4.73 (m, 2H), 4.54–4.49 (m, 1H), 4.41–4.38 (m, 1H), 3.34 (s, 3H), 3.10–2.95 (m, 2H), 2.97 (s, 3H), 1.58–1.55 (d, J = 7.5 Hz, 3H); ^{13}C NMR (100 MHz, $CDCl_3$): δ 166.55, 165.16, 163.02 (d, J = 245 Hz, 1C), 144.07, 138.88, 137.31, 135.68, 135.22, 129.14, 128.61, 128.18, 127.94, 127.86, 126.78, 124.21, 115.42, 115.21, 70.36, 53.86, 52.30, 49.26, 37.76, 37.55, 35.73, 21.66; LCMS (ESI): 610.1 $[M + H]^+$; HRMS: calcd for $C_{29}H_{32}N_7O_5FSNa$ 632.2067, found $C_{29}H_{32}N_7O_5FSNa$ 632.2097; $[\alpha]_D^{15} = -301.8^\circ$ (c 0.22, $CHCl_3$).

4.2.13. N^1-((R)-1-(4-Fluorophenyl)ethyl)-N^3-((2S,3S)-3-hydroxy-1-phenyl-4-(2H-tetrazol-2-yl)butan-2-yl)-5-(N-methylmethylsulfonamido)isophthalamide (**24**)

^{1}H NMR (300 MHz, CD_3OD): δ 9.07 (s, 1H), 8.09 (s, 1H), 7.99 (s, 1H), 7.87 (s, 1H), 7.44–7.40 (m, 2H), 7.31–7.22 (m, 4H), 7.18–7.16 (m, 1H), 7.08–7.02 (t, J = 8.4 Hz, 2H), 5.24–5.22 (q, J = 7.2 Hz, 1H), 4.68–4.61 (m, 1H), 4.51–4.42 (m, 2H), 4.18–4.13 (m, 1H), 3.35 (s, 3H), 3.10–2.95 (m, 2H), 2.97 (s, 3H), 1.58–1.56 (d, J = 7.2 Hz, 3H); ^{13}C NMR (100 MHz, $CDCl_3$): δ 166.18, 164.95, 163.09 (d, J = 245 Hz, 1C), 142.00, 138.62, 137.19, 135.58, 135.22, 129.18, 128.64, 128.02, 127.90, 127.75, 126.80, 124.25, 115.48, 115.27, 69.94, 56.99, 53.85, 49.12, 37.84, 37.69, 35.48, 21.58; LCMS (ESI): 610.2 $[M + H]^+$; HRMS: calcd for $C_{29}H_{32}N_7O_5FSNa$ 632.2067, found $C_{29}H_{32}N_7O_5FSNa$ 632.2065; $[\alpha]_D^{15} = -188.1^\circ$ (c 0.26, $CHCl_3$).

4.2.14. N^1-((R)-1-(4-Fluorophenyl)ethyl)-N^3-((2S,3S)-3-hydroxy-4-(4-(hydroxyl methyl)-1H-pyrazol-1-yl)-1-phenylbutan-2-yl)-5-(N-methylmethylsulfonamido)isophthalamide (**25**)

Compound **25** was obtained from **6** and (1H-pyrazol-4-yl) methanol (74 mg, 0.75 mmol) according to the similar procedure used to prepare **20**. The crude product was purified by silica gel chromatography to afford **25** (118 mg, 74.2%). ^{1}H NMR (300 MHz, $CDCl_3$): δ 8.01 (s, 1H), 7.94 (s, 1H), 7.82 (s, 1H), 7.43 (s, 1H), 7.36–7.32 (m, 3H), 7.28–7.21 (m, 2H), 7.20–7.19 (m, 1H), 7.08–6.96 (m, 4H), 5.29–5.27 (q, J = 7.2 Hz, 1H), 4.48 (s, 2H), 4.39–4.36 (m, 1H), 4.13–4.02 (m, 3H), 3.33 (s, 3H), 3.05–3.02 (m, 2H), 2.86 (s, 3H), 1.59–1.56 (d, J = 7.2 Hz, 3H); ^{13}C NMR (100 MHz, $CDCl_3$): δ 165.70, 164.66, 163.18 (d, J = 245 Hz, 1C), 142.14, 139.03, 138.56, 137.38, 135.91, 135.45, 129.69, 129.21, 128.51, 127.88, 127.45, 126.74, 123.98, 121.52, 115.63, 115.42, 71.42, 56.00, 55.10, 53.78, 48.90, 38.10, 37.91, 35.38, 21.75; LCMS (ESI): 637.2 $[M + H]^+$; HRMS: calcd for $C_{32}H_{36}N_5O_6FNaS$ 660.2268, found $C_{32}H_{36}N_5O_6FNaS$ 660.2257; $[\alpha]_D^{15} = -34.0^\circ$ (c 0.20, $CHCl_3$).

4.2.15. Ethyl-1-((2S,3S)-3-(3-((R)-1-(4-fluorophenyl)ethylcarbamoyl)-5-(N-methylmethylsulfonamido)benzamido)-2-hydroxy-4-phenylbutyl)-1H-pyrazole-4-carboxylate (**28**)

Compound **28** was obtained from **6** and ethyl 1*H*-pyrazole-4-carboxylate (105 mg, 0.75 mmol) according to the similar procedure used to prepare **20**. The crude product was purified by silica gel chromatography to afford **28** (122 mg, 76.6%). ^{1}H NMR (300 MHz, CD_3OD): δ 8.14 (s, 1H), 8.11 (s, 1H), 7.98 (s, 1H), 7.88 (s, 1H), 7.84 (s, 1H), 7.45–7.39 (m, 2H), 7.28–7.20 (m, 4H), 7.16–7.14 (m, 1H), 7.08–7.02 (t, J = 9.0 Hz, 2H), 5.24–5.22 (q, J = 6.6 Hz, 1H), 4.42–4.40 (m, 1H), 4.28–4.21 (m, 1H), 4.26–4.23 (q, J = 6.9 Hz, 2H), 4.15–4.12 (m, 2H), 3.35 (s, 3H), 3.05–2.98 (m, 2H), 2.95 (s, 3H), 1.58–1.55 (d, J = 6.6 Hz, 3H), 1.33–1.28 (t, J = 6.9 Hz, 3H); ^{13}C NMR (100 MHz, $CDCl_3$): δ 165.90, 164.67, 163.07 (d, J = 245 Hz, 1C), 160.64, 142.09, 141.24, 138.62, 137.30, 135.72, 135.30, 133.82, 129.21, 128.59, 127.88, 127.54, 126.61, 123.99, 115.55, 115.22, 114.85, 70.41, 60.34, 56.00, 55.76, 53.70, 49.03, 37.82, 35.41, 21.43, 14.15; LCMS (ESI): 680.2 $[M + H]^+$; HRMS: calcd for $C_{34}H_{39}N_5O_7FS$ 680.2554, found $C_{34}H_{39}N_5O_7FS$ 680.2546; $[\alpha]_D^{15} = -72.7^\circ$ (c 0.30, $CHCl_3$).

4.2.16. N^1-((2S,3S)-4-(4-Carbamoyl-1H-pyrazol-1-yl)-3-hydroxy-1-phenylbutan-2-yl)-N^3-((R)-1-(4-fluorophenyl)ethyl)-5-(N-methylmethylsulfonamido)isophthalamide (**30**)

Two equivalent NaOH (80 mg, 2 mmol) was dissolved in the solvent of THF/EtOH/H_2O = 2/2/1, then compound **28** (670 mg, 1 mmol) was added into the solution. The reaction was heated to reflux for 2 h. Then the PH was adjusted to 4 by diluted HCl, and extracted by EtOAc (30 mL × 2) and washed with saturated brine once (50 mL) sequentially. The organic layers were dried over Na_2SO_4, filtered and evaporated to give the crude product acid **29**, which was used directly in the next step. To a solution of the above acid (65 mg, 0.10 mmol) in 2 mL DMF was added ammonium chloride (6.0 mg, 0.11 mmol), HOBt (18 mg, 0.132 mmol), DIPEA (45 μL, 0.30 mmol) and stirred for 10 min. EDCI (25 mg, 0.132 mmol) was added and the mixture was allowed to react overnight at room temperature. Then the resulting mixture was diluted by 30 mL EtOAc and washed with diluted aqueous HCl aqueous (30 mL), dilute aqueous $NaHCO_3$ (30 mL) and saturated brine (30 mL) sequentially. The organic layers were dried over Na_2SO_4, filtered and evaporated to give the crude product amide, which was purified by silica gel chromatography to afford the target compound **30** (55 mg, 84.2%). ^{1}H NMR (300 MHz, CD_3OD): δ 8.13 (s, 1H), 8.10 (s, 1H), 7.99 (s, 1H), 7.89 (s, 2H), 7.44–7.40 (m, 2H), 7.28–7.20 (m, 4H), 7.16–7.14 (m, 1H), 7.07–7.02 (t, J = 6.3 Hz, 2H), 5.24–5.21 (q, J = 6.9 Hz, 1H), 4.44–4.39 (m, 1H), 4.32–4.26 (m, 1H), 4.14–4.11 (m, 2H), 3.34 (s, 3H), 3.09–2.98 (m, 2H), 2.95 (s, 3H), 1.58–1.56 (d, J = 6.9 Hz, 3H); ^{13}C NMR (100 MHz, $CDCl_3$) δ 166.12, 165.11, 163.17, 160.75 (d, J = 245 Hz, 1C), 141.84, 139.16, 138.73, 137.52, 135.86, 135.37, 132.92, 129.14, 128.52, 127.74, 126.64, 124.52, 123.94, 117.05, 115.61, 115.14, 70.65, 56.12, 53.94, 49.12, 37.89, 35.46, 29.65, 21.52; LCMS (ESI): 651.1 $[M + H]^+$; HRMS: calcd for $C_{32}H_{35}N_6O_6FNaS$ 673.2221, found $C_{32}H_{35}N_6O_6FNaS$ 673.2234; $[\alpha]_D^{15} = -135.0^\circ$ (c 0.08, $CHCl_3$).

4.2.17. N^1-((R)-1-(4-Fluorophenyl)ethyl)-N^3-((2S,3S)-3-hydroxy-4-(4-(methyl carbamoyl)-1H-pyrazol-1-yl)-1-phenylbutan-2-yl)-5-(N-methylmethylsulfonamido)isophthalamide (**31**)

Compound **31** was obtained from **29** and methylamine hydrochloride (7.5 mg, 0.11 mmol) according to the similar procedure used to prepare **30**. The crude product was purified by silica gel chromatography to afford **31** (53 mg, 80.1%). ^{1}H NMR (300 MHz, CD_3OD): δ 8.14 (s, 1H), 8.06 (s, 1H), 7.99 (s, 1H), 7.89 (s, 1H), 7.83 (s, 1H), 7.45–7.40 (m, 2H), 7.28–7.20 (m, 4H), 7.16–7.14 (m, 1H), 7.08–7.02 (t, J = 8.7 Hz, 2H), 5.24–5.22 (q, J = 7.2 Hz, 1H), 4.40–4.38 (m, 1H), 4.31–4.25 (m, 1H), 4.16–4.11 (m, 2H), 3.34 (s, 3H), 3.09–3.01 (m, 2H), 2.82 (s, 3H), 2.98 (s, 3H), 1.58–1.56 (d, J = 7.2 Hz, 3H); ^{13}C NMR (100 MHz, $CDCl_3$): δ 166.15, 165.08, 163.74, 162.92 (d, J = 245 Hz, 1C), 141.93, 139.43, 138.80, 137.81, 135.63, 135.22, 132.06, 129.28, 128.43, 128.27, 127.99, 126.46, 124.31, 117.89, 115.26, 115.05, 70.58, 54.13, 51.15, 49.23, 42.32, 37.86, 35.63, 26.10, 21.99; LCMS (ESI): 665.2 $[M + H]^+$; HRMS: calcd for $C_{33}H_{37}N_6O_6FNaS$ 687.2377, found $C_{33}H_{37}N_6O_6FNaS$ 687.2390; $[\alpha]_D^{15} = -68.8^\circ$ (c 0.26, $CHCl_3$).

4.2.18. N^1-((2S,3S)-4-(4-(Dimethylcarbamoyl)-1H-pyrazol-1-yl)-3-hydroxy-1-phenylbutan-2-yl)-N^3-((R)-1-(4-fluorophenyl)ethyl)-5-(N-methylmethylsulfonamido)isophthalamide (**32**)

Compound **32** was obtained from **29** and dimethylamine hydrochloride (9.0 mg, 0.11 mmol) according to the similar procedure used to prepare **30**. The crude product was purified by silica gel chromatography to afford **32** (53 mg, 78.4%). ^{1}H NMR (300 MHz, CD_3OD): δ 8.11 (s, 1H), 8.03 (s, 1H), 7.98 (s, 1H), 7.89 (s, 1H), 7.77 (s, 1H), 7.45–7.40 (m, 2H), 7.28–7.20 (m, 4H), 7.16–7.14 (m, 1H), 7.08–7.03 (t, J = 8.7 Hz, 2H), 5.24–5.22 (q, J = 6.9 Hz, 1H), 4.43–4.37 (m, 1H), 4.31–4.25 (m, 1H), 4.15–4.12 (m, 2H), 3.35 (s, 3H), 3.22 (s, 3H), 3.03 (s, 3H), 3.05–2.97 (m, 2H), 2.95 (s, 3H), 1.58–1.56 (d, J = 6.9 Hz,

3H); ^{13}C NMR (100 MHz, $CDCl_3$): δ 166.08, 164.83, 164.74, 163.03 (d, J = 245 Hz, 1C), 142.00, 139.46, 138.91, 138.88, 137.57, 135.76, 135.28, 129.20, 128.56, 127.92, 127.84, 126.62, 124.14, 116.76, 115.38, 115.17, 70.53, 56.02, 53.83, 48.97, 39.10, 37.84, 35.97, 35.52, 21.60; LCMS (ESI): 679.2 $[M + H]^+$; HRMS: calcd for $C_{34}H_{39}N_6O_6FNaS$ 701.2534, found $C_{34}H_{39}N_6O_6FNaS$ 701.2547; $[\alpha]_D^{15} = -43.0^\circ$ (*c* 0.30, $CHCl_3$).

*4.2.19. N^1-((2S,3S)-4-(4-(Diethylcarbamoyl)-1H-pyrazol-1-yl)-3-hydroxy-1-phenylbutan-2-yl)-N^3-((R)-1-(4-fluorophenyl)ethyl)-5-(N-methylmethylsulfonamido)isophthalamide (**33**)*

Compound **33** was obtained from **29** and diethylamine (8.0 mg, 0.11 mmol) according to the similar procedure used to prepare **30**. The crude product was purified by silica gel chromatography to afford **33** (57 mg, 81.0%). ^{1}H NMR (300 MHz, CD_3OD): δ 8.11 (s, 1H), 7.98 (s, 2H), 7.90 (s, 1H), 7.72 (s, 1H), 7.45–7.40 (m, 2H), 7.27–7.19 (m, 4H), 7.16–7.08 (m, 1H), 7.04–7.03 (t, J = 8.7 Hz, 2H), 5.24–5.22 (q, J = 6.9 Hz, 1H), 4.42–4.37 (m, 1H), 4.31–4.25 (m, 1H), 4.18–4.13 (m, 2H), 3.50 (s, 4H), 3.35 (s, 3H), 3.05–2.98 (m, 2H), 2.97 (s, 3H), 1.58–1.56 (d, J = 6.9 Hz, 3H), 1.20 (s, 6H); ^{13}C NMR (100 MHz, $CDCl_3$): δ 166.16, 164.85, 163.95, 163.08 (d, J = 245 Hz, 1C), 142.05, 138.89, 138.70, 137.58, 135.87, 135.27, 133.03, 129.24, 128.58, 127.93, 127.85, 126.65, 124.07, 117.25, 115.43, 115.22, 70.48, 55.92, 54.03, 50.60, 49.01, 37.87, 37.72, 35.53, 21.65, 12.99; LCMS (ESI): 707.2 $[M + H]^+$; HRMS: calcd for $C_{36}H_{43}N_6O_6FNaS$ 729.2847, found $C_{36}H_{43}N_6O_6FNaS$ 729.2834; $[\alpha]_D^{15} = -26.3^\circ$ (*c* 0.40, $CHCl_3$).

*4.2.20. N^1-((R)-1-(4-Fluorophenyl)ethyl)-N^3-((2S,3S)-3-hydroxy-1-phenyl-4-(4-(pyrrolidine-1-carbonyl)-1H-pyrazol-1-yl)butan-2-yl)-5-(N-methylmethylsulfonamido)isophthalamide (**34**)*

Compound **34** was obtained from **29** and pyrrolidine (8.0 mg, 0.11 mmol) according to the similar procedure used to prepare **30**. The crude product was purified by silica gel chromatography to afford **34** (52 mg, 74.1%). ^{1}H NMR (300 MHz, CD_3OD): δ 8.12–8.10 (m, 2H), 7.99 (s, 1H), 7.89 (s, 1H), 7.85 (s, 1H), 7.45–7.40 (m, 2H), 7.25–7.20 (m, 4H), 7.16–7.14 (m, 1H), 7.08–7.03 (t, J = 8.7 Hz, 2H), 5.24–5.22 (q, J = 6.9 Hz, 1H), 4.40–4.38 (m, 1H), 4.30–4.27 (m, 1H), 4.16–4.13 (m, 2H), 3.69–3.68 (m, 2H), 3.56–3.51 (t, J = 6.9 Hz, 2H), 3.35 (s, 3H), 3.04–2.98 (m, 2H), 2.95 (s, 3H), 1.99–1.91 (m, 4H), 1.58–1.56 (d, J = 6.9 Hz, 3H); ^{13}C NMR (100 MHz, $CDCl_3$): δ 165.98, 164.80, 163.06, 162.50 (d, J = 245 Hz, 1C), 142.03, 139.48, 138.92, 137.57, 135.79, 135.29, 133.67, 129.24, 128.58, 127.86, 127.73, 126.64, 124.15, 117.85, 115.41, 115.20, 70.47, 56.16, 53.88, 49.00, 48.32, 46.92, 37.87, 35.53, 23.95, 21.65; LCMS (ESI): 705.4 $[M + H]^+$; HRMS: calcd for $C_{36}H_{42}N_6O_6FS$ 705.2871, found $C_{36}H_{42}N_6O_6FS$ 705.2884; $[\alpha]_D^{15} = -50.4^\circ$ (*c* 0.25, $CHCl_3$).

*4.2.21. N^1-((R)-1-(4-Fluorophenyl)ethyl)-N^3-((2S,3S)-3-hydroxy-1-phenyl-4-(4-(piperidine-1-carbonyl)-1H-pyrazol-1-yl)butan-2-yl)-5-(N-methylmethylsulfonamido)isophthalamide (**35**)*

Compound **35** was obtained from **29** and piperidine (9.0 mg, 0.11 mmol) according to the similar procedure used to prepare **30**. The crude product was purified by silica gel chromatography to afford **35** (56 mg, 78.2%). ^{1}H NMR (300 MHz, CD_3OD): δ 8.12 (s, 1H), 7.98 (s, 1H), 7.95 (s, 1H), 7.89 (s, 1H), 7.68 (s, 1H), 7.45–7.40 (m, 2H), 7.27–7.20 (m, 4H), 7.16–7.14 (m, 1H), 7.08–7.03 (t, J = 8.1 Hz, 2H), 5.25–5.22 (q, J = 7.5 Hz, 1H), 4.40–4.39 (m, 1H), 4.30–4.24 (m, 1H), 4.15–4.12 (m, 2H), 3.66–3.62 (m, 4H), 3.35 (s, 3H), 3.06–2.97 (m, 2H), 2.95 (s, 3H), 1.70–1.60 (m, 6H), 1.58–1.56 (d, J = 7.5 Hz, 3H); ^{13}C NMR (100 MHz, $CDCl_3$): δ 166.11, 164.77, 163.43, 163.13 (d, J = 245 Hz, 1C), 142.09, 138.93, 137.57, 135.84, 135.30, 132.81, 129.25, 128.61, 127.95, 127.88, 127.79, 126.68, 124.04, 116.87, 115.48, 115.27, 70.50, 57.62, 55.92, 54.01, 49.01, 37.91, 37.77, 35.57, 26.35, 24.43, 21.68; LCMS (ESI): 719.3 $[M + H]^+$; HRMS: calcd for $C_{37}H_{44}N_6O_6FS$ 719.3027, found $C_{37}H_{44}N_6O_6FS$ 719.3014; $[\alpha]_D^{15} = -44.1^\circ$ (*c* 0.27, $CHCl_3$).

*4.2.22. N^1-((R)-1-(4-Fluorophenyl)ethyl)-N^3-((2S,3S)-3-hydroxy-4-(4-(morpholine-4-carbonyl)-1H-pyrazol-1-yl)-1-phenylbutan-2-yl)-5-(N-methylmethylsulfonamido)isophthalamide (**36**)*

Compound **36** was obtained from **29** and morpholine (10.0 mg, 0.11 mmol) according to the similar procedure used to prepare **30**. The crude product was purified by silica gel chromatography to afford **36** (51 mg, yield: 71.3%). ^{1}H NMR (300 MHz, CD_3OD): δ 8.11–8.10 (m, 1H), 7.99–7.98 (m, 2H), 7.90–7.89 (m, 1H), 7.72 (s, 1H), 7.45–7.40 (m, 2H), 7.28–7.20 (m, 4H), 7.17–7.14 (m, 1H), 7.08–7.03 (t, J = 6.9 Hz, 2H), 5.24–5.22 (q, J = 6.9 Hz, 1H), 4.39–4.35 (m, 1H), 4.30–4.24 (m, 1H), 4.15–4.12 (m. 2H), 3.71–3.65 (m, 8H), 3.35 (s, 3H), 3.04–2.98 (m, 2H), 2.95 (s, 3H), 1.58–1.56 (d, J = 6.9 Hz, 3H); ^{13}C NMR (100 MHz, $CDCl_3$) δ 165.98, 164.62, 163.50, 160.67 (d, J = 245 Hz, 1C), 142.12, 139.20, 138.67, 137.38, 135.71, 135.27, 132.86, 129.24, 128.67, 127.95, 127.61, 126.77, 123.98, 116.26, 115.56, 115.34, 70.49, 66.67, 55.92, 55.87, 53.92, 49.05, 45.74, 37.88, 35.38, 21.69; LCMS (ESI): 721.3 $[M + H]^+$; HRMS: calcd for $C_{36}H_{41}N_6O_7FSNa$ 743.2639, found $C_{36}H_{41}N_6O_7FSNa$ 743.2684; $[\alpha]_D^{15} = -100.5^\circ$ (*c* 0.21, $CHCl_3$).

*4.2.23. N^1-((2S,3S)-4-(4-(Azepane-1-carbonyl)-1H-pyrazol-1-yl)-3-hydroxy-1-phenylbutan-2-yl)-N^3-((R)-1-(4-fluorophenyl)ethyl)-5-(N-methylmethylsulfonamido)isophthalamide (**37**)*

Compound **37** was obtained from **29** and azepane (11.0 mg, 0.11 mmol) according to the similar procedure used to prepare **30**. The crude product was purified by silica gel chromatography to afford **37** (59 mg, yield: 81.2%). ^{1}H NMR (300 MHz, CD_3OD): δ 8.12 (s, 1H), 7.98 (s, 2H), 7.90 (s, 1H), 7.73 (s, 1H), 7.45–7.40 (m, 2H), 7.25–7.20 (m, 4H), 7.16–7.14 (m, 1H), 7.08–7.03 (t, J = 8.4 Hz, 2H), 5.24–5.22 (q, J = 6.9 Hz, 1H), 4.40–4.35 (m, 1H), 4.30–4.25 (m, 1H), 4.16–4.12 (m, 2H), 3.70–3.66 (t, J = 6.0 Hz, 2H), 3.62–3.58 (t, J = 6.0 Hz, 2H), 3.35 (s, 3H), 3.04–2.98 (m, 2H), 2.95 (s, 3H), 1.77 (s, 4H), 1.58 (s, 4H), 1.58–1.56 (d, J = 6.9 Hz, 3H); ^{13}C NMR (100 MHz, $CDCl_3$): δ 166.10, 164.82, 164.56, 163.09 (d, J = 245 Hz, 1C), 142.06, 139.09, 138.90, 137.56, 135.86, 135.28, 133.23, 129.25, 128.60, 127.94, 127.72, 126.66, 124.05, 117.35, 115.44, 115.23, 70.46, 55.98, 53.99, 49.06, 46.43, 37.87, 35.53, 29.63, 27.24, 26.71, 21.67; LCMS (ESI): 733.4 $[M + H]^+$; HRMS: calcd for $C_{38}H_{46}N_6O_6FS$ 733.3184, found $C_{38}H_{46}N_6O_6FS$ 733.3148; $[\alpha]_D^{15} = -46.0^\circ$ (*c* 0.20, $CHCl_3$).

4.3. Enzyme-based assay of BACE1 and cathepsin D

Recombinant human β-secretase ectodomain (amino acid residues 1–460) was expressed as a secreted protein with a C-terminal His tag in insect cells using baculovirus infection. The BACE activity was determined at room temperature by monitoring the hydrolysis of FRET substrate DABCYL-Ser-Glu-Val-Asn-Leu-Asp-Ala-Glu-Phe-EDANS (SynPep Corp, USA). In a typical 100 μL assay mixture containing 100 mM ammonium acetate, pH 4.0, 20 μM substrate, and 50 nM purified recombinant human BACE1/Fc, the enzyme activity was continuously monitored with excitation 355 nm/emission 460 nm filter set for 20 min and the initial rate of the hydrolysis was determined using the early linear region of the enzymatic reaction kinetic curve.

Cathepsin D activity was measured in 100 mM formate buffer, pH 3.1, using Mca-GKPILFFRLK(DNP)-*D*-R-NH_2 (2 μM). Test substances were serially diluted from 10 μM to 10 nM, inhibition assays were done in black 96-wellplates (Costar) by adding the respective enzyme in assay buffer. Plates were incubated at room temperature for 1 h, and residual enzymatic activity was measured after addition of substrate in a Spectramax Gemini fluorescence plate reader (Molecular Devices, Sunnyvale, CA). IC_{50} values were calculated using the Microsoft Excel extension XL-fit.

4.4. Cellular Aβ lowering assay in APP transfected HEK293

Human embryonic kidney 293 cell transfected with APP695 cDNA containing the Swedish double mutation (HEK293sw), a line known for its tendency to generate high level of aggregating Aβ, was used to examine the effects of the compounds on BACE1 activity. HEK293sw cells were seeded into 6-well plates with a total volume of 1.5 mL of the cell suspension in Dulbecco's modified Eagle medium (DMEM, Gibco), supplemented with 10% (v/v) heat inactivated Fetal bovine serum. In the meantime, different concentrations of the compounds were added to the cultures and incubated for 24 h at 37 °C and 5% CO_2. The conditioned medium was removed from the culture wells and $A\beta_{1-40}$ peptide levels in the media were analyzed by Human β Amyloid 1–40 Colorimetric Elisa kit (BioSource International, Inc. California, USA) after 24 h.

4.5. Protein purification and crystallization

A detailed description of production of recombinant human BACE1 has been done in our previous publication [21]. Briefly, BACE1 was expressed in *Escherichia coli* as inclusion bodies that were then denatured and refolded into the active monomer. A cDNA fragment encoding BACE1 residues 43–454 was cloned into pET28a with a TEV protease cleavage site following a six-residue His-Tag added at the N-terminus. After refolding, nickel beads (Ni Sepharose™ High Performance, Amersham Biosciences, Uppsala, Sweden) were used to concentrate the protein. The eluted BACE1 was then injected into a 124 mL Hiload Superdex75 column from which it was eluted with 1 mM DTT/0.5 M urea/150 mM NaCl/20 mM Tris–HCl, pH 7.5. In order to obtain crystals with different protein packing patterns, two mutations, K75A and E77A, were introduced into BACE1 together.

The active BACE1 monomer in the elution buffer was concentrated to 8–10 mg/mL. Cocrystallization of compound **12**, **20** and **28** with mutated BACE1 was performed at room temperature using the hanging drop vapor-diffusion method, by mixing the solution of the protein-compound complex with an equal volume of a precipitant solution, 1.7 M Li_2SO_4/100 mM HEPES, pH 7.5. The protein-compound complex was prepared by adding the compound to the protein solution to reach a final concentration of 0.5 mM ligand. The perfluoropolyether, PFO-X175/08 (Hampton Research), was used as cryoprotectant for all the crystals.

Table 4
Data collection and refinement statistics.

	Compound **12**	Compound **20**	Compound **28**
Pdb code	3UQX	3UQU	3UQW
Space group	$C222_1$	$C222_1$	$C222_1$
Cell dimensions			
a (Å)	104.55	104.47	107.32
b (Å)	128.28	128.24	131.54
c (Å)	76.39	76.18	78.54
Wavelength (Å)	0.9792	0.9791	1.0089
Reflections[a]	56,267 [53,400]	56,630 [53,726]	28,642 [27,042]
Resolution range (Å)	1.70–81.04	1.70–80.99	2.20–83.15
Highest-resolution shell (Å)	1.70–1.73	1.70–1.73	2.20–2.24
Redundancy[b]	13.5 (7.2)	11.2 (8.1)	10.6 (9.8)
$I/\sigma(I)$[b]	27.7 (3.67)	40.99 (7.54)	11.53 (4.92)
Completeness (%)[b]	99.0 (89.2)	99.7 (97.6)	100.0 (100.0)
R_{work}/R_{free} (%)[b]	15.89/18.62	16.32/19.50	17.51/20.69
RMS values			
Bond length (Å)	0.031	0.031	0.029
Bond angle (°)	2.820	2.753	2.088
Number of non-hydrogen atoms			
Protein	2944	2918	2888
Inhibitor	46	43	48
Water oxygen	322	309	143
Others	$3SO_4^{2+}$, 7URE, $2CL^-$	$3SO_4^{2+}$, 2URE, $1CL^-$	$2SO_4^{2+}$
Mean temperature factors ($Å^2$)			
Protein	15.24	15.43	30.50
Inhibitor	13.71	16.62	33.61
Ramachandran plot			
Residues in most-favored regions	345 (95.57%)	351 (96.43%)	351 (95.38%)
Residues in allowed regions	15 (4.16%)	12 (3.30%)	16 (4.35%)
Residues in disallowed regions	1 (0.28%)	1 (0.27%)	1 (0.27%)

[a] The numbers in parenthese are the numbers of unique reflections.
[b] The numbers in brackets correspond to the highest resolution shells.

4.6. Structure determination and refinement

Data were collected at 100 K on beamline BL17U (at wavelength 0.9793 Å) at the Shanghai Synchrotron Radiation Facility (SSRF) (Shanghai, China) for the co-crystallized structures. The data were processed with the HKL2000 [22], software packages, and the structures were then solved by molecular replacement, using the CCP4 program MOLREP [23]. The search model used for the crystals was the apo wild type BACE1 structure (PDB ID code: 3TPL). The structures were refined using the CCP4 program REFMAC5 [23] combined with the simulated-annealing protocol implemented in the program PHENIX [24]. With the aid of the program Coot [25], compound, water molecules, and others were fitted into to the initial F_o-F_c maps. The complete statistics, as well as the quality of the solved structures, are shown in Table 4.

Acknowledgments

This work was financially supported by the National S&T Major Projects "Key New Drug Creation and Manufacturing Program" of China (Grant Nos. 2009ZX09301-001, and 2009ZX09501-010), the "100 Talents Project" of CAS (to Y. X.), the Shanghai Pujiang Program (Grant No. 10PJ1412000), and the National Natural Science Foundation of China (Grant No. 21172233).

Appendix A. Supplementary data

Supplementary data related to this article can be found at http://dx.doi.org/10.1016/j.ejmech.2013.06.027.

References

[1] (a) Alzheimer's Association, 2010 Alzheimer's disease facts and figures, Alzheimers Dement. 6 (2010) 158–194;
(b) H.W. Querfurth, F.M.N. LaFerla, Mechanisms of disease: Alzheimer's disease, Engl. J. Med. 326 (2010) 329–344;
(c) C. Mount, C. Downton, Alzheimer disease: progress or profit? Nat. Med. 12 (2006) 780–784;
(d) C. Ferri, M. Prince, C. Brayne, H. Brodaty, L. Fratiglioni, M. Ganguli, K. Hall, K. Hasegawa, H. Hendrie, Y. Huang, A. Jorm, C. Mathers, P.R. Menezes, E. Rimmer, M. Scazufca, Global prevalence of dementia: a Delphi consensus study, Lancet 366 (2005) 2112–2117.
[2] J. Hardy, D.J. Selkoe, The amyloid hypothesis of Alzheimer's disease: progress and problems on the road to therapeutics, Science 297 (2002) 353–356.
[3] S. Sinha, I. Lieberburg, Colloquium paper: cellular mechanisms of β-amyloid production and secretion, Proc. Natl. Acad. Sci. U. S. A. 96 (1999) 11049–11053.
[4] (a) G.T. Wong, D. Manfras, F.M. Poulet, Q. Zhang, H. Josien, T. Bara, L. Engstrom, M. Pinzon-Ortiz, J.S. Fine, H.-J.J. Lee, L. Zhang, G.A. Higgins, E.M. Parker, Chronic treatment with the γ-secretase inhibitor LY-411, 575 inhibits β-amyloid peptide production and alters lymphopoiesis and intestinal cell differentiation, J. Biol. Chem. 279 (2004) 12876–12882;
(b) J. Milano, J. McKay, C. Dagenais, L. Foster-Brown, F. Pognan, R. Gadient, R.T. Jacobs, A. Zacco, B. Greenberg, P.J. Ciaccio, Modulation of notch processing by γ-secretase inhibitors causes intestinal goblet cell metaplasia and induction of genes known to specify gut secretory lineage differentiation, Toxicol.

Sci. 82 (2004) 341–346;
(c) G.H. Searfoss, W.H. Jordan, D.O. Calligaro, E.J. Galbreath, L.M. Schirtzinger, B.R. Berridge, H. Gao, M.A. Higgins, P.C. May, T.P. Ryan, Adipsin, a biomarker of gastrointestinal toxicity mediated by a functional γ-secretase inhibitor, J. Biol. Chem. 278 (2003) 46107–46116;
(d) P. Doerfler, M.S. Shearman, R.M. Perlmutter, Presenilin-dependent γ-secretase activity modulates thymocyte development, Proc. Natl. Acad. Sci. U. S. A. 98 (2001) 9312–9317;
(e) B.K. Hadland, N.R. Manley, D.-M. Su, G.D. Longmore, C.L. Moore, M.S. Wolfe, E.H. Schroeter, R. Kopan, γ-Secretase inhibitors repress thymocyte development, Proc. Natl. Acad. Sci. U. S. A. 98 (2001) 7487–7491.

[5] H. Cai, Y. Wang, D. McCarthy, H. Wen, D.R. Borchelt, D.L. Price, P.C. Wong, BACE1 is the major β-secretase for generation of A peptides by neurons, Nat. Neurosci. 4 (2001) 233–234.

[6] Y. Luo, B. Bolon, S. Kahn, B.D. Bennett, S. Babu-Khan, P. Denis, W. Fan, H. Kha, J. Zhang, Y. Gong, L. Martin, J.C. Louis, Q. Yan, W.G. Richards, M. Citron, R. Vassar, Mice deficient in BACE1, the Alzheimer's β-secretase, have normal phenotype and abolished β-amyloid generation, Nat. Neurosci. 4 (2001) 231–232.

[7] S.L. Roberds, J. Anderson, G. Basi, M.J. Bienkowski, D.G. Branstetter, K.S. Chen, S.B. Freedman, N.L. Frigon, D. Games, K. Hu, K. Johnson-Wood, K.E. Kappenman, T.T. Kawabe, I. Kola, R. Kuehn, M. Lee, W. Liu, R. Motter, N.F. Nichols, M. Power, D.W. Robertson, D. Schenk, M. Schoor, G.M. Shopp, M.E. Shuck, S. Sinha, K.A. Svensson, G. Tatsuno, H. Tintrup, J. Wijsman, S. Wright, L. McConlogue, BACE knockout mice are healthy despite lacking the primary β-secretase activity in brain: implications for Alzheimer's disease therapeutics, Hum. Mol. Genet. 10 (2001) 1317–1324.

[8] (a) J. Hardy, The membrane cytoskeletal protein adducin is phosphorylated by protein kinase C in D1 neurons of the nucleus accumbens and dorsal striatum following cocaine administration, J. Neurochem. 110 (2009) 1129–1137;
(b) T.E. Golde, D. Dickson, M. Hutton, Filling the gaps in the Aβ cascade hypothesis of Alzheimer's disease, Curr. Alzheimer Res. 3 (2006) 421–426;
(c) W.L. Klein, G.A. Krafft, C.E. Finch, Targeting small Aβ oligomers: the solution to an Alzheimer's disease conundrum? Trends Neurosci. 24 (2001) 219–224;
(d) J.A. Hardy, G.A. Higgins, Alzheimer's disease: the amyloid cascade hypothesis, Science 256 (1992) 184–185.

[9] L. Hong, G. Koelsch, X. Lin, S. Wu, S. Terzyan, A.K. Ghosh, X.C. Zhang, J. Tang, Structure of the protease domain of memapsin 2 (β-secretase) complexed with inhibitor, Science 290 (2000) 150–153.

[10] (a) Ellen W. Baxter, Kelly A. Conway, Ludo Kennis, François Bischoff, Marc H. Mercken, Hans L. De Winter, Charles H. Reynolds, Brett A. Tounge, Chi Luo, Malcolm K. Scott, Yifang Huang, Mirielle Braeken, Serge M.A. Pieters, Didier J.C. Berthelot, Stefan Masure, Wouter D. Bruinzeel, Alfonzo D. Jordan, Michael H. Parker, Robert E. Boyd, Junya Qu, Richard S. Alexander, Douglas E. Brenneman, Allen B. Reitz, 2-Amino-3,4-dihydroquinazolines as inhibitors of BACE-1 (β-Site APP cleaving enzyme): use of structure based design to convert a micromolar hit into a nanomolar lead, J. Med. Chem. 50 (2007) 4261–4264;
(b) Philip D. Edwards, Jeffrey S. Albert, Mark Sylvester, David Aharony, Donald Andisik, Owen Callaghan, James B. Campbell, Robin A. Carr, Gianni Chessari, Miles Congreve, Martyn Frederickson, Rutger H.A. Folmer, Stefan Geschwindner, Gerard Koether, Karin Kolmodin, Jennifer Krumrine, Russell C. Mauger, Christopher W. Murray, Lise-Lotte Olsson, Sahil Patel, Nate Spear, Gaochao Tian, Application of fragment-based lead generation to the discovery of novel, cyclic amidine β-secretase inhibitors with nanomolar potency, cellular activity, and high ligand efficiency, J. Med. Chem. 50 (2007) 5912–5925. Danzhi Huang, Urs Lüthi, Peter Kolb, Marco Cecchini, Alcide Barberis, Amedeo Caflisch, In silico discovery of β-secretase inhibitors, J. Am. Chem. Soc. 128 (2006) 5436–5443.

[11] Shawn J. Stachel, Craig A. Coburn, Thomas G. Steele, Kristen G. Jones, Elizabeth F. Loutzenhiser, Alison R. Gregro, Hemaka A. Rajapakse, Ming-Tain Lai, Ming-Chih Crouthamel, Min Xu, Katherine Tugusheva, Janet E. Lineberger, Beth L. Pietrak, Amy S. Espeseth, Xiao-Ping Shi, Elizabeth Chen-Dodson, M. Katharine Holloway, Sanjeev Munshi, Adam J. Simon, Lawrence Kuo, Joseph P. Vacca, Structure-based design of potent and selective cell-permeable inhibitors of human β-secretase (BACE-1), J. Med. Chem. 47 (2004) 6447–6450.

[12] Lawrence R. Marcin, Mendi A. Higgins, F. Christopher Zusi, Yunhui Zhang, Michael F. Dee, Michael F. Parker, Jodi K. Muckelbauer, Daniel M. Camac, Paul E. Morin, Vidhyashankar Ramamurthy, Andrew J. Tebben, Kimberley A. Lentz, James E. Grace, Jovita A. Marcinkeviciene, Lisa M. Kopcho, Catherine R. Burton, Donna M. Barten, Jeremy H. Toyn, Jere E. Meredith, Charles F. Albright, Joanne J. Bronson, John E. Macor, Lorin A. Thompson, Synthesis and SAR of indole-and 7-azaindole-1,3-dicarboxamide hydroxyethylamine inhibitors of BACE-1, Bioorg. Med. Chem. Lett. 21 (2001) 537–541.

[13] Michel C. Maillard, Roy K. Hom, Timothy E. Benson, Joseph B. Moon, Shumeye Mamo, Michael Bienkowski, Alfredo G. Tomasselli, Danielle D. Woods, D. Bryan Prince, Donna J. Paddock, Thomas L. Emmons, John A. Tucker, Michael S. Dappen, Louis Brogley, Eugene D. Thorsett, Nancy Jewett, Sukanto Sinha, Varghese John, Design, synthesis, and crystal structure of hydroxyethyl secondary amine-based peptidomimetic inhibitors of human β-secretase, J. Med. Chem. 50 (2007) 776–781.

[14] Stacey R. Lindsley, Keith P. Moore, Hemaka A. Rajapakse, Harold G. Selnick, Mary Beth Young, Hong Zhu, Sanjeev Munshi, Lawrence Kuo, Georgia B. McGaughey, Dennis Colussi, Ming-Chih Crouthamel, Ming-Tain Lai, Beth Pietrak, Eric A. Price, Sethu Sankaranarayanan, Adam J. Simon, Guy R. Seabrook, Daria J. Hazuda, Nicole T. Pudvah, Jerome H. Hochman, Samuel L. Graham, Joseph P. Vaccaa, Philippe G. Nantermet, Design, synthesis, and SAR of macrocyclic tertiary carbinamine BACE-1 inhibitors, Bioorg. Med. Chem. Lett. 17 (2007) 4057–4061.

[15] Yiping Zhu, Kun Xiao, Lanping Ma, Bin Xiong, Yan Fu, Haiping Yu, Wei Wang, Xin Wang, Dingyu Hu, Hongli Peng, Jingya Li, Qi Gong, Qian Chai, Xican Tang, Haiyan Zhang, Jia Li, Jingkang Shen, Design, synthesis and biological evaluation of novel dual inhibitors of acetylcholinesterase and β-secretase, Bioorg. Med. Chem. 17 (2009) 1600–1613.

[16] H.C. Kolb, K.B. Sharpless, The growing impact of click chemistry on drug discovery, Drug Discov. Today 8 (2003) 1128–1137.

[17] (a) P. Wu, A.K. Feldman, A.K. Nugent, C.J. Hawker, A. Scheel, B. Voit, J. Pyun, J.M.J. Fre chet, K.B. Sharpless, V.V. Fokin, Efficiency and fidelity in a click-chemistry route to triazole dendrimers by the copper(I)-catalyzed ligation of azides and alkynes, Angew. Chem. Int. Ed. 43 (2004) 3928–3932;
(b) M.V. Gil, M.J. Ar evalo, O. Lopez, Click chemistry – what's in a name? Triazole synthesis and beyond, Synthesis 11 (2007) 1589–1620.

[18] (a) V.V. Rostovtsev, L.G. Green, V.V. Fokin, K.B. Sharpless, A stepwise Huisgen cycloaddition process: copper(I)-catalyzed regioselective "ligation" of azides and terminal alkynes, Angew. Chem. Int. Ed. 41 (2002) 2596–2599;
(b) H.C. Kolb, M.G. Finn, K.B. Sharpless, Click chemistry: diverse chemical function from a few good reactions, Angew. Chem. Int. Ed. 40 (2001) 2004–2021.

[19] Fu-Sen Liang, Ashraf Brik, Ying-Chuan Lin, John H. Elder, Chi-Huey Wonga, Epoxide opening in water and screening in situ for rapid discovery of enzyme inhibitors in microtiter plates, Bioorg. Med. Chem. 14 (2006) 1058–1062.

[20] Fredrik Wångsell, Karin Gustafsson, Ingemar Kvarnstro, Neera Borkakoti, Michael Edlund, Katarina Jansson, Jimmy Lindberg, Anders Hallberg, Åsa Rosenquist, Bertil Samuelsson, Synthesis of potent BACE-1 inhibitors incorporating a hydroxyethylene isostere as central core, Eur. J. Med. Chem. 45 (2010) 870–882.

[21] Y. Xu, M. Li, H. Greenblatt, W. Chen, A. Paz, O. Dym, Y. Peleg, T. Chen, X. Shen, J. He, H. Jiang, I. Silman, J.L. Sussman, Flexibility of the flap in the active site of BACE1 as revealed by crystal structures and molecular dynamics simulations, Acta Crystallogr. D68 (2012) 13–25.

[22] Z. Otwinowski, W. Minor, Processing of X-ray diffraction data collected in oscillation mode, Macromol. Crystallogr. Part A (1997) 307–326.

[23] M.D. Winn, C.C. Ballard, K.D. Cowtan, E.J. Dodson, P. Emsley, P.R. Evans, R.M. Keegan, E.B. Krissinel, A.G.W. Leslie, A. McCoy, S.J. McNicholas, G.N. Murshudov, N.S. Pannu, E.A. Potterton, H.R. Powell, R.J. Read, A. Vagin, K.S. Wilson, Overview of the CCP 4 suite and current developments, Acta Crystallogr. D67 (2011) 235–242.

[24] P.D. Adams, R.W. Grosse-Kunstleve, L.-W. Hung, T.R. Ioerger, A.J. McCoy, N.W. Moriarty, R.J. Read, J.C. Sacchettini, N.K. Sauter, T.C. Terwilliger, PHENIX: building new software for automated crystallographic structure determination, Acta Crystallogr. D58 (2002) 1948–1954.

[25] P. Emsley, K. Cowtan, Coot: model-building tools for molecular graphics, Acta Crystallogr. D60 (2004) 2126–2132.